ASSESSMENT OF NATURAL RADIO ACTIVITY CONCENTRATION LEVELS IN GEOLOGICAL SAMPLES COLLECTED IN SELECTED AREAS IN MAKUENI COUNTY

MUTUNGA JAMES MUTUNGI

I56/CE/22274/2012

A Thesis Submitted in Partial Fulfillment of the Requirements for the Award of the Degree of Master of Science (Physics) in the School of Pure and Applied Sciences of Kenyatta University.

November, 2018

DECLARATION

This Thesis is my original work and has not been presented for any academic award in any university.

Signature:..... Date :21/11/2018

MUTUNGA JAMES MUTUNGI - 156/CE/22274/2012

Department of physics

SUPERVISORS

We confirm that the work reported in this thesis was carried out by the candidate under our own supervision

Signature:..... Date:24/11/2018

Dr. Nadir Hashim

Department of Physics

Kenyatta University

Signature:..... Date :21/11/2018

Dr. Charles Migwi

Department of Physics

Kenyatta University

DEDICATION

I thank the almighty lord for his care during my research period**.** I dedicate my work to my wife Jacinta Mutungi and son Francis Musyoka.

ACKNOWLEDGEMENTS

I sincerely thank my research supervisors, Dr Nadir O Hashim and Dr Charles Migwi for their professional guidance throughout my research work. My gratitude goes also to the chairman and the entire staff of the physics department Kenyatta University, for their intellectual support during the writing of this work. I would also like to appreciate the support of my family who supported me financially and morally. My gratitude also goes to the chief technician physics department Kenyatta University for his great support during my research work. I also thank most sincerely the technical team in the department of geography Kenyatta University for their assistance in the drawing of the required map. My special thanks go to Mutuku Ndete who was my help during the collection of the samples. I cannot forget to thank my colleagues, Enock Musamali, Tirus Njuguna and Elijah Kirui for their support during the research. Sincere thanks to my wife Jacinta Mutungi for the encouragement and every kind of support during my research period.

TABLE OF CONTENTS

LIST OF TABLES

LIST OF FIGURES

LIST OF ABBREVIATIONS AND ACRONYMS

A.D.C	Analogue to digital converter
DNA	Deoxyribonucleic acid
EPA	Environmental Protection Agency
EP	Energy peak
FWHM	Full wavelength at half maximum
GOK	Government Of Kenya
GPS	Global Positioning System
IAEA	International Atomic Energy Agency
ICRP	International Commission On Radiological Protection
IPNI	International Plant Nutrition Institute
MCA	Multichannel Analyzer
MCB	Multichannel Buffer
MDA	Minimum detectable activity
NaI(Tl)	Sodium Iodide Thallium activated detector
NEMA	National Environmental Management Authority
PMT	Photomultiplier tube
UNSCEAR	United Nations Scientific Committee On Effects Of Atomic Radiations
UNEP	United Nations Environmental Programme
UK	United Kingdom
WHO	World Health Organization

ABSTRACT

Natural radiation is the major contributor to the external dose and varies depending on the radioactivity concentration of naturally occurring radionuclides and their decay products in soil and rocks. Exposure to a high dose to human beings leads to health problems. Assessment of natural radioactivity concentration levels in geological samples collected in selected areas of Makueni County was carried out using gamma ray spectroscopy technique. Spectrum decomposition method was used to decompose the measured gamma ray spectra into spectral components of separate radionuclides. The measured peak intensities were used to calculate the activity concentration of the radionuclides in the samples. The average concentrations of ^{238}U, ^{232}Th and ^{40}K measured in the soil samples collected in this study were 69 ± 5 $BqKg^{-1}$,53 ± 3 $BqKg^{-1}$ and 1098 ± 69 $BqKg^{-1}$ respectively while rocks were found to have concentrations of 139 ± 6 $BqKg^{-1}$, 73 ± 3 $BqKg^{-1}$, $1573 \pm 65$$BqKg^{-1}$ respectively. On average both rocks and soils were found to have activity concentrations of 104 ± 5 $BqKg^{-1}$, 63 ± 3 $BqKg^{-1}$, 1336 ± 67 $BqKg^{-1}$ for ^{238}U, ^{232}Th and ^{40}K respectively. These values are above the global average values. To measure radiation hazard to the public, absorbed dose rate in air at a height of 1m above the ground surface was estimated. Absorbed dose rate in rocks was 175 ± 7 $nGyh^{-1}$ while in soil it was found to be 110 ± 7 $nGyh^{-1}$ These values are higher than the world average of 60 $nGyh^{-1}$ (UNSCEAR, 2002).The effective dose rate calculated for human exposure from the ionizing radiations of ^{238}U,^{232}Th and^{40}K in the soil samples collected were found to have 0.29 ± 0.02 $mSvy^{-1}$ while rocks registered 0.45 ± 0.02 $mSvy^{-1}$ These health hazard parameters were below the safe limit of 1.0 $mSvy^{-1}$ (ICRP, 1991; UNSCEAR, 2002) and therefore do not indicate significant health hazard for the inhabitants of the selected area. The building materials from the study area are safe for use and I recommend that the government and other non- governmental organizations use this study as a baseline study in radioactivity concentration levels of the area.

CHAPTER ONE

INTRODUCTION

1.1 Background of the study

Many studies on radiological survey using gamma ray spectrometry have been done around the world. The main aim is to provide data that can be used for environmental radiations monitoring and underground gas and oil exploration. The knowledge of the distribution of these radionuclides is very important in estimating the level of natural background radiation to which humans are exposed (Termizi *et al*., 2005).

The exposure to ionizing radiations is carcinogenic since the radiations attack the D.N.A of a living cell. One of the somatic effects to the irradiated cell is the development of solid tumours in the skin, bone, lung, thyroid and the breast (IAEA, 2005).These tumours are cancerous.

Cancer is generic term used for a group of diseases characterized by the growth and spread of abnormal cells beyond their usual boundaries (GOK: Kenya National Cancer Control Strategy Report, 2017-2022) .One of the risk factors is the ionizing radiations. Globally cancer is the second leading cause of death while in Kenya; it's in the third position (GOK: Kenya National Cancer Control Strategy Report, 2017-2022).

Many countries have formulated policies towards the realization of a cancer free environment and Kenya is among these countries. Through the ministry of health various reports and policies have been released. In Makueni county ,the County government published the Makueni County Cancer Control Act in 2016 (Makueni County Gazette Supplement no:20,Acts no 6 ,2016),This was to set up an institute mandated with the establishment of measures that seek to eradicate conditions that cause and aggravate the spread of cancer in the county.

The irradiation of a cell by an ionizing radiation may be as a result of natural sources in the environment such as radon gas present in the underground mines or cosmic radiation and man- made sources such as radioactive sources in the nuclear industry and X-Ray machines in the health care (Cancers due to ionizing radiation report, U.K Government, 2016).

It is therefore important to closely monitor the ionization radiation levels from natural and artificial sources of ionizing radiations. This study was aimed at estimating levels of human exposure to ionizing radiations to residents in selected areas of Makueni County Kenya.

1.1.1 Geology of Makueni County

Makueni County is bounded by the latitudes $1^0$30'S and 3^0 00'S and longitudes 37^0 00'E and 38^0 00'E.A large portion of the county is predominated by the basement rock. This consists of the crystalline limestone, the quartzite intertwined with the muscovite schist and the hornblende bearing gneisses (Geology of the South- East Machakos Area 1953 reprint 2007; Geology Of Simba- Kibwezi Area, 1963).

The granite rock is traced in various areas within the county, this include the Ithumba hill in the Nguu division. Other traces of the granite rocks are found in the Mbooni hills, Taiti hill in Kalamba division. The granite rocks are associated with radioactive elements (Hashim, 2001).The metamorphosed rocks such as the granitoid gneiss is clearly visible along the Muooni River near Emali town. The gneiss rock is also available in the Kyemundu hills.

Matha hill in the Nzaui region has an outcrop of the pyrtiferon calc-silicate gneiss rock on its upper slopes. The quartzite schist has high levels of radionuclide concentration. The basic intrusive rock in this region is the amphibolite and the pyroxenite these form the volcanic rock which runs through the western part of the county.

Notable towns along this volcanic rock belt are Sultan- Hamud, Emali, Kiboko and Kibwezi. The red soil is used for making rough bricks which are used for building of houses and shops at town centers. Sand is readily available in this county. The black cotton soil is available in certain parts of the county .The soil is sticky when wet and when dry it's hard and characterized by contraction cracks. It's black in colour.

1.1.2 Environmental radionuclides

Environmental radioactivity occurs in two forms: Natural and Artificial. Natural radiation consists of cosmic radiation and terrestrial radiation. In cosmic radiation Cosmogenic radionuclides such as ^{3}H, ^{7}Be, ^{14}C and ^{22}Na are as a result of the interaction of primary cosmic-ray particles (mainly high–energetic photons) from their sources like the sun, black holes, supernovae and nebulae in the outer space with atoms in the earth's atmosphere. This generates secondary cosmic ray particles which propagate to reach the earth's atmosphere and because of their high energies they are detected on the surface of the earth (Grupen, 2005; Hayakawa, 1969). Secondary cosmic radiation consists of neutrons, protons, kaons, electrons and muons; Natural radiation is the largest contributor to external radiation source in the world's population (UNSCEAR, 2000).

Terrestrial radiation in the environment is largely due to uranium and thorium decay series since ^{238}U and ^{232}Th are radioactive. Merrie and Thomas (1997) and (Chozzi *et al.,* 2000) observed that the abundance of ^{238}U is 99.28% which implies that the contribution of ^{238}U to external radiation dose is very high in the environment.

Another naturally occurring radionuclide is the ^{40}K, these three radionuclides ^{238}U, ^{232}Th and ^{40}K, are the main contributors to the dose from natural radiation. The half-lives of these radionuclides are into the order of hundreds of millions of years and their distribution depends on the distribution of rocks from which they originate (Mohanty *et al*., 2004)

Artificially produced radionuclides are as a result of atmospheric-weapon testing, accidental and routine emissions (UNSCEAR, 1993). In general 80% of total annual radiation dose rate received per year by the general public is from natural sources and the largest component of this is radon gas and its decay products in the indoor environment. The percentage contribution of ionizing radiation exposed to humans is shown in figure 1.1

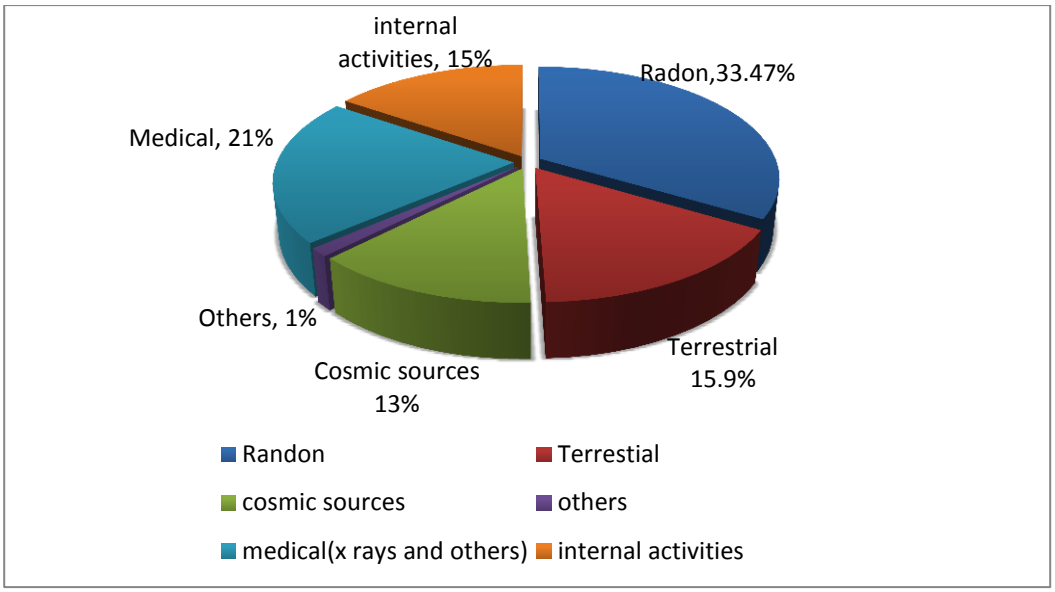

Figure1.1: Typical human exposure to natural and artificial sources of radiation (Clark *et al.*, 1997; W.H.O, 2012)

Radon with an exposure of 33.47% is an intermediate step in the normal radioactive decay chain through which thorium and uranium decay to lead.

1.2 Statement of the problem

Rocks and soil are used as building materials by humans, but the risks associated with the exposure to the ionization radiation from the naturally occurring radionuclide materials (NORM) are not very well studied in Kenya. This is also the trend in all other parts of the world. It is therefore difficult to arrive at a global

value for parameters such as dose rate (UNSCEAR, 2000). The inhabitants of Makueni County rely on rocks and soil from the region for construction of their houses. Rocks are used for the construction of the walls in the permanent houses while bricks made from soil of this region are used for walling purposes for semi-permanent houses.

The walls of the traditional houses in this region are constructed using mud (semi-liquid mixture of soil and water) and supported by wooden trunks. These traditional houses have no cemented floor, only soil is spread and watered for the soil particles to be joined.

This research therefore aims at assessing the possible health risks which the inhabitants of the selected areas of Makueni County continue to expose themselves to from the naturally occurring radionuclides from these building materials. It also determines whether the measured radiation doses are within the safe limits.

1.3 Objectives

1.3.1 General objective

The general objective of this study is to assess human radiation exposure to natural radiation sources for the soil and rocks in selected areas of Makueni County.

1.3.2 Specific objectives

1) To determine the radioactivity concentration levels of naturally occurring radionuclides: ^{238}U, ^{232}Th and ^{40}K, present in the rock and soil samples collected from selected areas in Makueni County.
2) To calculate the radiological parameters like absorbed gamma radiation dose rate, effective dose rate and radium equivalent activity due to rock and soil samples.

3) To estimate radiological hazards by calculating dose to risk conversion, internal radiation hazard index, external radiation hazard index, alpha index and the representative level index.

1.4 Rationale of the research

Radiation emission information is useful to provide awareness in the general public concerning the health risks involved in exposure to ionizing radiations. Few studies on natural radioactivity and indoor radon concentration measurements have been reported (Hashim, 2001; Chege, 2007).

Rocks and soil from Makueni County are used for building and construction. The selected region has rapidly growing towns like Emali along Mombasa-Nairobi highway and Matiliku town which have a high demand for building rocks and soil, not forgetting the growing demand of houses in the homesteads due to the ever growing population, but despite the use of these building materials from this region, there is no available data on the radiological hazards and health risks which the inhabitants of this region continue to expose themselves to.

The data obtained in this research is timely and will be used to create public awareness on health risks due to exposure to ionizing radiations and be part of the baseline data that can be used by future researchers in radiation field. Environmental agencies either governmental like N.E.M.A or non-governmental like U.N.E.P will use the data of this research to formulate policies regarding environmental health in Makueni County.

CHAPTER TWO

LITERATURE REVIEW

2.1 Introduction

Natural radioactivity is the spontaneous disintegration of an unstable radioactive atomic nucleus releasing radiation and energy. The radiations released are: Alpha particle and the beta particle while the energy is in the form of gamma rays. Exposure to these gamma rays has health effects to the human body both long term and short term. Natural radioactivity in parts of Kenya and other areas in the world have been studied by many researchers. Depending on where the research is conducted the researchers have given the levels of radioactivity concentration in those areas and made specific conclusions basing on their findings. In this chapter studies on natural radioactivity in Kenya and outside Kenya are given a review.

2.2 Studies on natural radioactivity outside Kenya

In a study to determine natural radioactivity concentration levels in soil samples along the Amman Aqaba highway in Jordan it was found that the concentration levels were: 22-104Bq/kg, 21-103Bq/kg and 138-601Bq/kg for ^{238}U, ^{232}Th and ^{40}K respectively. The highest value of concentration of ^{238}U was obtained from a site which was very close to a phosphate mine (Jundi *at al.,* 2003). However from this study the effective dose rate per year of 40-151 μSvy^{-1} was within the accepted limit of $1mSvy^{-1}$ for members of public.

In Kuwait Natural radioactivity concentration levels in sediments along the coastal strip were analyzed. The concentration levels, in the southern coastal strip, of ^{238}U of 13.5 ± 6.2 Bq/kg were higher than in the northern coastal strip and this was attributed to the deposition of volatile depleted uranium (Saad H.R and Al-Azmi, 2002).

A research on natural radioactivity due to dissolved radon contents in the deep continental intercalaire aquifer of Algeria and Tunisia gave an activity of 3-32 Bq/L; this was attributed to the presence of sandstones which contain terrestrial radionuclides (Trevor *et al*., 2014).

A study on natural radioactivity and radiological hazards in soil and phosphate samples in Aswan area Egypt found that the concentration of ^{226} Ra,^{232} Th and ^{40}K ranged between 59 $\pm$6.7 to 638 $\pm$31.0 Bq/kg, 9.9 $\pm$1.4 to 406 $\pm$6.3 Bq/kg, 213 $\pm$9.5 to 798 $\pm$30.6 Bq/kg respectively (Harb *et al.,* 2008).

Evaluation of NORM and Dose assessment in an aluminum industry in Nigeria found that radium equivalent activity is within the acceptable limits of 370 Bq/Kg (Janet *et al.,* 2013).

In Tripoli metropolitan Libya, surface soils were measured for radioactivity concentration using gamma ray spectrometry, the findings show concentration of 10.5 Bq/Kg, 9.5 Bq/Kg, 270 Bq/Kg for ^{238}U, ^{232}Th,^{40}K (Shenber, 1996).

A research on phosphate rocks collected from Minjungu mines in Tanzania for measurements on radioactivity show that there is a high concentration of ^{226}Ra of 5760 $\pm$ 107 Bqkg^{-1} in phosphate rock. The concentration of wild leaf vegetation is 650$\pm$11Bqkg^{-1}, edible leaf 393$\pm$9 Bqkg^{-1} and in chicken feed 4.0$\pm$0.1 Bqkg$^{-1,}$ these findings suggest a health risk when there an ingestion of the samples (Banzi *et al.,* 2000).

2.3 Studies on natural radio activity in Kenya

Radioactivity concentration levels in surface soils around titanium mines in Kwale County, Kenya, was studied and found that the mean levels of ^{232}Th, ^{226}Ra and ^{40}K are below the global average (Osoro, 2007).

In a study on natural radioactivity and elemental concentration in Mombasa Island, It was found that the north and the south coast of Kenya the dose rate was below the safe limit of 1 $mSvy^{-1}$for members of public (Hashim, 2001).

Gamma ray spectrometric analysis of sediment deposits at the shores of Lake Nakuru found that the activity concentration of ^{238}U,^{232}Th and^{40}K being higher than those reported in other areas in Kenya.The range is 36.9 $\pm$ 9.1, 43.5 $\pm$ 3.8 and 708.3 $\pm$ 33.2 Bq/kg respectively (Langat, 2009).

Soil samples from Mrima hills in Taita-Taveta County, Kenya were measured for natural radioactivity concentration levels .The average absorbed dose rate was found to be 440.7 $nGyh^{-1}$, (Kebwaro, 2009) this is higher than the world's average concentration of 60$nGyh^{-1}$(UNSCEAR, 2000).

In a study on natural radioactivity and elemental concentration levels in soil, rocks and water samples from Kibwezi district, Makueni County it was found that the concentrations of ^{238}U, ^{232}Th and ^{40}K is 130.6 $\pm$ 38.7Bq/kg, 137.9 $\pm$ 39.7 Bq/kg, 1120.1 $\pm$ 245.2 Bq/kg. Absorbed radiation dose rate in air from terrestrial gamma rays ranged from 95.4 $\pm$ 3.2 $nGyh^{-1}$ to 300.4 $\pm$5.5 $nGyh^{-1}$ with an average of 193.2 $\pm$ 44.5nGy^{-1} (Mutie, 2011).

This study provides current information on assessment of natural radioactivity concentration levels and radiological risks which the inhabitants of the selected areas of Makueni County (Former Nzaui district) continue to expose themselves to despite the use of these materials from this area.

2.4 Naturally occurring radionuclides

Natural radionuclides on the earth exist in three categories.

1) **Primordial radionuclides** –These radionuclides have been in existence on the Earth's surface for a long time ago. They are found in the igneous rock and

sedimentary rock which readily available in the environment and with time they also dissolve in water, or escape to the air as radon gas.

2) **Cosmogenic radionuclides**-They originate from cosmic ray particles interaction in the outer space .The sun and other heavenly bodies are sources of

these radionuclides. Since they are energetic they generate secondary particles in the space which penetrate the atmosphere to reach the Earth's surface.

3) **Human produced radionuclides**-These are due to the human activity like body imaging using radioactive elements or using uranium rods to generate electricity.

All these radionuclides are available in air, water, soil, rocks and fruits from plants growing in areas with these radionuclides (Berezniki *et al*.,1990).The primordial radionuclides that are common are ^{238}U,^{232}Th and^{40}K (UNSCEAR, 2000). They have half-life comparable to the age of the earth.

2.5 Man-made radionuclides in the environment

Manmade radionuclides are as a result of human activities and especially in the field of nuclear technology. The most common radionuclides are ^{137}Cs and ^{90}Sr (Clark *et al*., 1997). These radionuclides are mainly introduced in the environment through the following ways:

a) Weapon testing in deserts or oceans waters.
b) Fission and fusion reactors in the search for a reliable source of power and energy to sustain the ever-growing demand for more industries due to the growing population.
c) In medicine for example in the treatment of the thyroid glands ($^{131}\mathbf{I}$)

2.6 Biological effects of radionuclides

Gamma radiation is mainly from radionuclides ^{238} U,^{232}Th,^{40} K .The radiations from these radionuclides include:-alpha particles,beta particles, and gamma radiations. The effects of ionizing radiations in body tissues are the creation of positron and electron pair which cause biological harm. These effects can be divided into two categories:

Somatic effects –These are the harm that an affected individual suffers during their life time e.g.: irradiation induced cancer, sterility and life shortening.

Genetic effects-These are radiation induced mutations to an individual genes and DNA that can contribute to the birth of defective descendants.

When the radiation dose is above 1 Sv, massive cell death and possibly death of the individual may occur (ICRP, 1991). Harmful effect of the addition of these radionuclides is categorized in to two categories

A) **Stochastic**-These are the effects where the probability of occurrence increases with the increasing dose but the severity doesn't depend on the dose and therefore no threshold is set worldwide since the radiation only affects a single cell.

B) **Deterministic Effect-**They have a dose threshold below which they cannot occur. The severity of the effect depends on the dose received. These include infertility in men, development of cataracts and even death (Andrew and Len, 1994).

To minimize the exposure effects ICRP has set exposure limits due to background and medicinal radiation.

Table 2.1 gives the exposure limits due to ionizing radiations.

Table 2.1: Annual radiation dose safe limits (ICRP, 2007)

Population group	**Dose limit($mSvy^{-1}$)**
Members of the public	5
Non classified workers	15
Classified workers	
Whole body	50
Feet	500
Eyes	150
hands	500

2.7 Absorbed dose

The amount of energy imparted to a particular volume of a material determines the whole biological effects. The dosimetric quantity in radiological protection is the absorbed dose (D) expressed as (IAEA, 2005)

$$D=\frac{d\varepsilon}{dm} \quad \ldots\ldots\ldots\ldots\ldots\ldots\ldots\ldots\ldots\ldots\ldots\ldots\ldots\ldots\ldots\ldots\ldots\ldots\ldots\ldots\ldots\ldots 2.1$$

where: D is the absorbed dose

$-d\varepsilon$ -is the sum of all the energy entering the volume of interest minus all energy leaving the volume, taking into account any mass–energy Conversion within the volume.

– dm - is the change in mass.

CHAPTER THREE

THEORETICAL CONCEPTS IN GAMMA RAY SPECTROMETRY

3.1 Introduction

Theoretical concepts in natural radioactivity, gamma ray emission and photon interaction with matter are presented in this chapter so as to give an in-depth knowledge on the ionizing radiations.

3.2 Gamma ray photon

A gamma ray photon is an energetic radiation with high penetration ability and ionizing power**.** There are two ways in which they are produced.

(i) In radioactive decay

(ii) A charged particle accelerating in an electric field-mostly accelerators.

During a radioactive decay an element decays into a daughter element by emission of either α, β^+ or β^- .This leaves the nuclide in the excited state, in order to achieve ground state it releases one or several γ-ray energy. An example of such a transition is illustrated in figure 3.1.

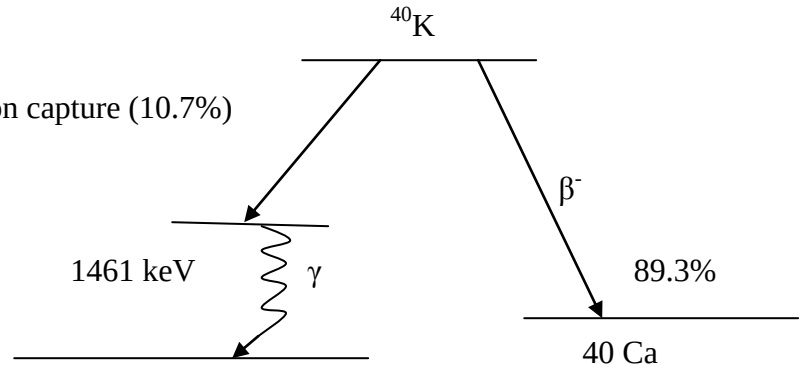

Fig 3.1: Decay scheme of ^{40} K.

^{40}K decays by releasing gamma ray energy in order to achieve its ground state. The half-life of ^{40}K is $1.3x10^9$ years it decays with 89.3% by emission of β^- to ^{40}Ca and 10.7% by the electron capture to an excited state of ^{40}Ar then decays later to its ground state by the emission of γ –ray energy of 1460keV.

3.3 Secular and transient equilibrium

The activity, A for a given number of atoms N of a given nuclide is given in equation 3.1.The rate of decay of a radionuclide is proportional to the number of atoms present.

$$\frac{dN}{\partial t} = -\lambda n = A \qquad (3.1)$$

where

λ - is the decay constant

The activity of radionuclide after time t is given by the equation 3.2

$$A = A_o e^{-\lambda t} \qquad (3.2)$$

In radioactivity an unstable nuclide undergoes spontaneous disintegration to achieve stability by emitting a radiation or a particle and giving stable daughter nuclei in the equation

$$A \longrightarrow B + X \qquad (3.3)$$

where A is the parent, B is the daughter and X is particle or a radiation.

<u>In secular equilibrium</u> $T_{B\ 1/2} << T_{A\ 1/2}$ and therefore $\frac{dNb}{dt} = \lambda_A N_A - \lambda_B N_B$ at secular equilibrium $\frac{dN}{dt} = 0$ and $N_B = \frac{\lambda A}{\lambda B} N_A$ (3.4)

<u>In transient equilibrium</u> $T_{B\ ½} < T_{A\ ½}$ (The half-life is not negligible).

where: $T_{A\ 1/2}$ & $T_{B\ 1/2}$ is the half-life of parent and daughter respectively.

3.4 PHOTON INTERACTION WITH MATTER

There are four ways in which a gamma ray photon can interact with matter: photoelectric absorption effect, Compton scattering, Rayleigh scattering and electron – positron pair production.

3.4.1 Photoelectric absorption effect

In photoelectric absorption effect or the photoelectric effect, the photon interacts with a tightly bound orbital electron of an atom and disappears, while the orbital electron is ejected from the atom as a photo- electron, with a kinetic energy E_k, given as (IAEA, 2005).

$$E_K = h\nu - E_B \quad (3.5)$$

where:

hν – is the energy of the incident photon

E_B - is the binding energy of the electron

E_K - is the kinetic energy of the ejected photo- electron.

The probability that an electron will undergo a photoelectric effect is expressed as a cross-section ${}_a\tau$, it varies with atomic number Z and the energy of the incident photon (hν)

where:

$${}_a\tau \propto z^n/(h\nu)^m \quad (3.6)$$

where, n and m are within the ranges of 3 to 5 depending on the energy of the incident photon and the mass of the atom. It's worth noting that heavier atoms absorbs gamma radiations more effectively as far as photo electric effect is concerned than light ones. Figure 3.2 shows a schematic illustration of the photoelectric absorption effect.

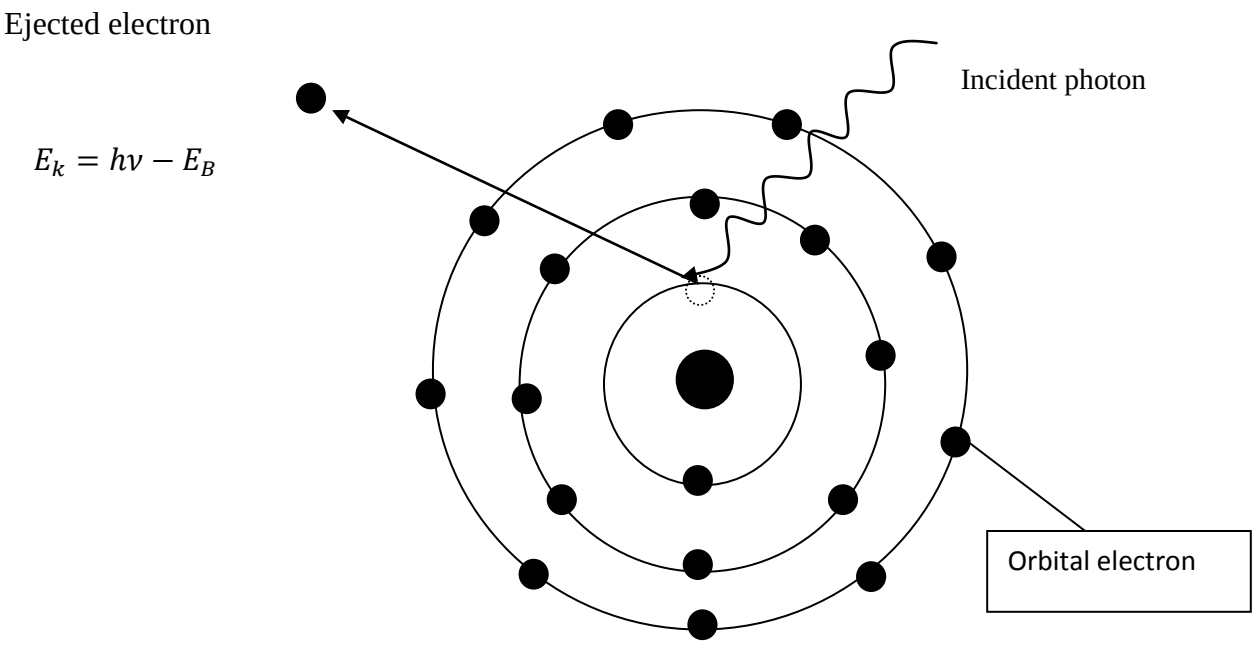

Fig 3.2: Photoelectric effect.

The incident photon interacts with an orbital electron, dislodging it from its energy shell. The ejected electron is called a photoelectron.

3.4.2 Compton scattering

In Compton scattering the incoming gamma ray photon is scattered through an angle θ with respect to its original direction. Because all angles of scattering are possible, the energy transferred can vary from zero to a large fraction of the gamma ray energy. The γ -ray can only transfer part of its energy to a recoil electron. The maximum transfer of energy to the transferring electron and hence the minimum energy of the scattered gamma, occurs when $\theta = 180^0$

The energy of the scattered photon is

$$h\nu' = \frac{h\nu}{1+\frac{h\nu}{MC}2(1-COS\theta)} \qquad (3.7)$$

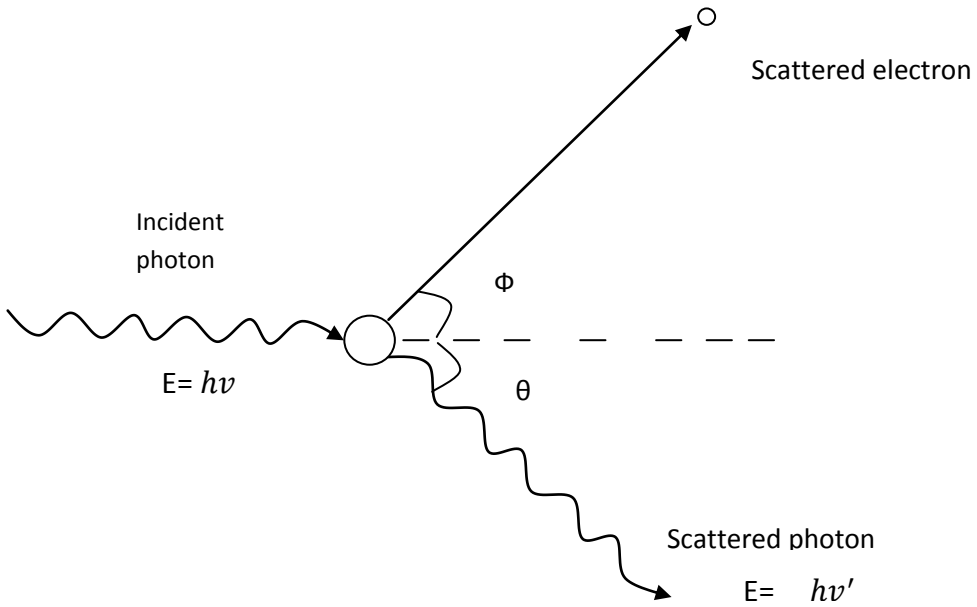

Fig 3.3. A schematic illustration of Compton scattering process (IAEA, 2005)

The incident photon with energy hv interacts with loosely bound electron and scattered at energy hv^1.The probability that an electron will undergo a Compton scattering is as a crossection ${}_e\sigma_c$ given as (IAEA, 2005).

$${}_a\sigma_c \propto \frac{z}{hv} \qquad (3.8)$$

This crossection increases linearly with the atomic number z of the absorber atom.

3.4.3 Rayleigh scattering

In Rayleigh scattering the incident photon interacts with a bound orbital electron. The event is elastic, hence the photon loses essentially none of its energy and it's scattered only through a small angle. Since no energy transfer occurs from the photon to the charged particles Rayleigh scattering plays no role in the energy transfer coefficient, however it contributes to the attenuation coefficient.

The crossection of interaction ${}_a\sigma_R$ is expressed as;

$${}_a\sigma_R \propto \left(\frac{Z}{h\nu}\right)^2 \quad (3.9)$$

3.4.4 Pair production

In pair production the photon completely disappears in the atom with photon energy equal to $h\nu \geq 2m_oc^2$ .Any excess photon energy is carried away by the electron, positron pair as kinetic energy. This energy is estimated to be 1022 keV (Gordon, 2008).The crossection of interaction ${}_ak$, varies as the square of the atomic number of the absorber material and its expressed as:

$${}_ak \propto z^2 \quad (3.10)$$

Figure 3.4 shows a schematic illustration of the pair production process.

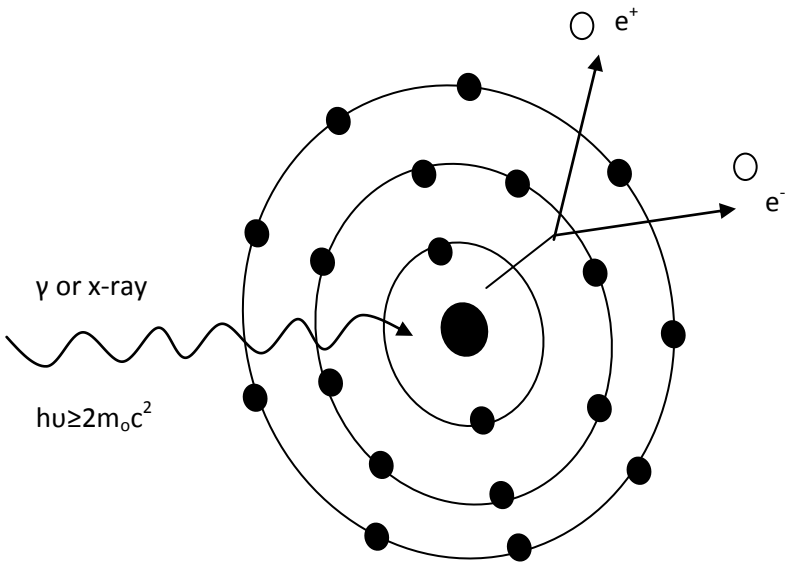

Fig 3.4: Schematic illustration of pair production process.

A photon with threshold energy equal to $h\upsilon \geq 2m_oc^2$completely disappears into the atom any excess energy is carried away by the positron electron pair as kinetic energy.

3.5 Relative predominance of individual effects

The probability for a photon to undergo any of the various interactions phenomena depends on the photon energy hν and the atomic number Z of the attenuating material(IAEA,2005).The graph in fig 3.5 shows the (Z,hv) relationship for a given material. The curve at the left display the regions where ${}_a\sigma_c={}_a\tau$ and the curve at the right display the region where ${}_a\sigma_c={}_ak$ .It is evident that photoelectric effect occurs at low photon energies, Compton scattering at intermediate energies while pair production occurs at high energies.

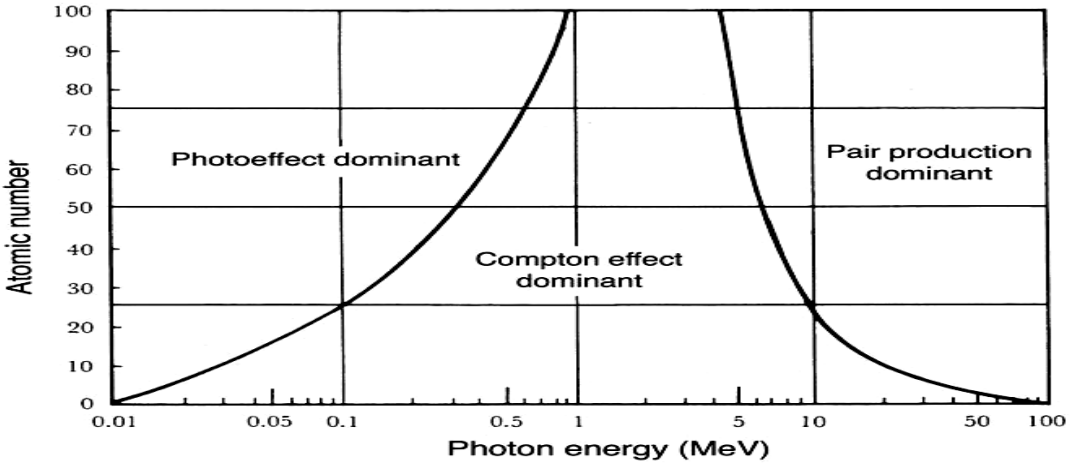

.

Fig 3.5: Predominance of the three main forms of photon interaction with matter (IAEA, 2005).

Photoelectric effect predominates at low photon energies, while pair production predominates at higher photon energies

3.6 Photon beam attenuation

The intensity of a photon beam for a given medium at a depth x is attenuated exponentially as follows:

$$I(x) = I_0 e^{(-\mu x)} \qquad (3.11)$$

where: I_0 – is the intensity of the incident radiation

μ-linear attenuation coefficient and depends on the photon energy, atomic number Z and density of the absorbing medium.

To avoid inconsistencies in measurement there should be uniform sample thickness around the detector.

CHAPTER FOUR

MATERIALS AND METHODS

4.1 Study Area

The study area lies in Makueni County .Its bounded by the latitudes $1^0 50^0$ S and $2^0 10^0$S and longitudes $37^0 30^0$ E and $37^0 45^0$ E. It was formerly called Nzaui district with its head- quarters at Matiliku Town. This region has hills like the Nzaui hill, Kyemundu hills and Nguu hill. The geology of the study area is covered under geology of Makueni County (section **1.1.1,** this thesis**).** In 2009 population and housing census, the district had a total population of 204,675 people (GOK: The 2009 Kenya Population and Housing Census Report). Rocks from this region are used for walling in permanent houses, while rough bricks make the walls of the semi- permanent houses (Geology of Simba- Kibwezi Area, 1963). Traditional houses are constructed using mud and tree trunks to offer support. Sand is available in rivers like Muooni, Kikuu, Maatini and their tributaries. The study area has three major towns: Emali, Matiliku, and Kalamba. There is a high demand of rocks and soil from this region due to the fast growing towns and the growing population in the quest for housing.

4.2 Sampling

The sampling points where in the Kalamba, Matiliku, Mbitini, Mulala and Nguu Divisions. Simple random method was applied in sampling to achieve statistical sensitivity (IAEA, 2004).Three samples were collected from each sampling point and mixed to produce a composite mixture for quality assurance. The geographical positions of the sampling points were determined by a hand held GPS machine. The samples were collected from sites which registered a reading above twenty c/s from the hand held radiation survey meter. It consisted of Geiger-Müller tube and a counter. Ten soil samples and ten rock samples were collected. Rock samples were chipped from unweathered rock in the hills, and along the rivers.

Soil samples were scooped from farms, grazing lands and forests. In each site for soil sample, vegetation and debris was removed to expose the soil and at a depth of about 20 to 23 cm soil sample was collected. Soil at this depth is considered as surface soil (I.P.N.I plant nutrition, 2008-2009 no.2). Each sample collected weighted approximately 500g.The figure 4.1 shows the study area map.

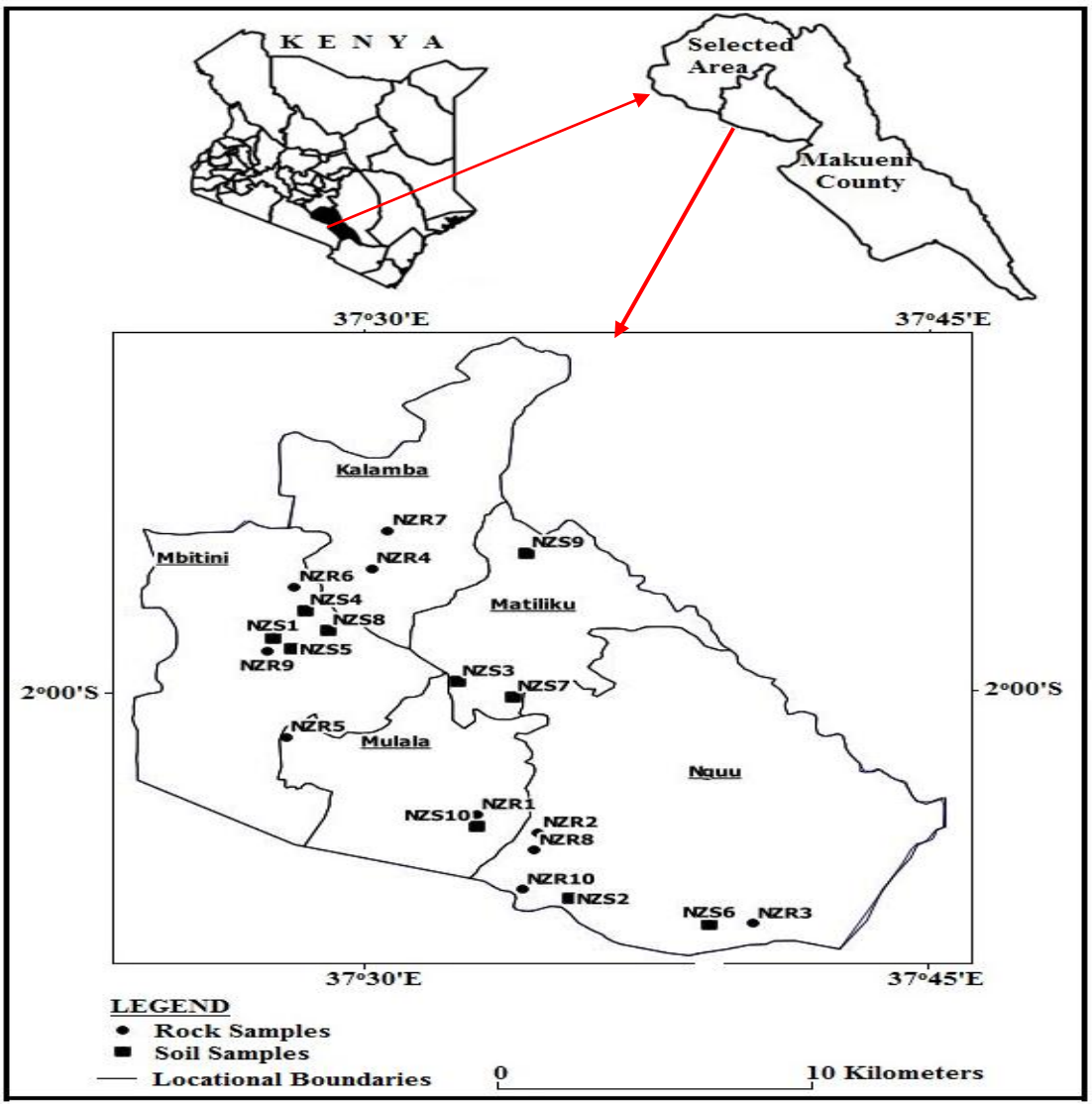

Fig 4.1: Map of study area (Survey of Kenya, 2009)

4.3 Sample preparation

Each rock and soil sample was sun dried in a dry weather for three days, they were then dried for 24 hours at 105 ^{0}C in an oven this was to ensure that the residual moisture is completely removed (Santawamaitre, 2012).The dried samples were pulverized using a motor and pestle manually and sieved through a 200 µm steel mesh for homogeneity.

Each sample was placed in a sealed plastic container to prevent the escape of the gaseous ^{222}Rn and ^{220} Rn; they were then labeled and stored for 30 days. This allows ^{238}U, ^{232}Th to reach secular equilibrium with their radionuclide daughters before measurement of radioactivity concentration levels (Termizi *et al*., 2005). Activity concentration of natural radionuclides was measured using a 76 mm x76 mm NaI (Tl) detector.

4.4 NaI (Tl) Gamma ray spectrometer

The gamma ray spectrometer used in this work consists of a shielded 76mm × 76mm NaI (TI) detector. The detecting system includes an Oxford PCA-P card operating on MS-DOS or Windows Operating System. The PCA-P contains a high voltage power supply, a charge sensitive preamplifier, a shaping amplifier, 80MHz Wilkinson analogue to digital converter (ADC) with multi-channel analyzer. The PCA-P card using a PC performs the data acquisition and analysis.. Radiations from the sample are detected by the spectrometer. The energetic electrons produced loose part of their energies through some scintillation mechanisms and the rest of the energies is converted into visible or near U.V photons. Figure 4.2 shows a schematic diagram of the NaI (TI) Spectrometer.

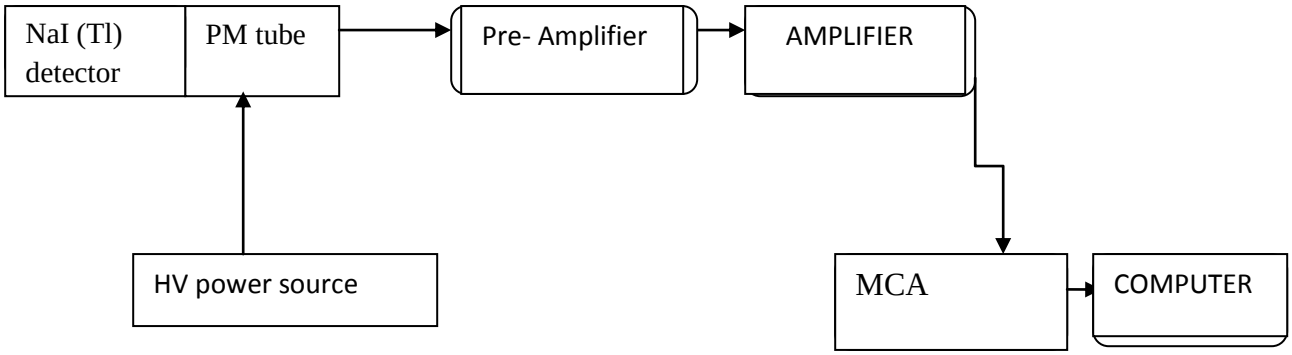

Fig 4.2: Schematic diagram of NaI (TI) Spectrometer.

The cathode in the scintillator liberates electrons by photoelectric effect. The liberated electrons are accelerated to the dynodes in the photomultiplier by E.H.T voltage supply in the PMT tube. An electron reaching one dynode produces secondary electron emission. This process is repeatedly done by the other dynodes and the resultant pulses are fed into multichannel analyzer (MCA) for analysis. The MCA records and stores pulses according to their energy values in the MCA channels. Collected data is stored in from a spectrum. A radioactive source produces gamma rays of various energies and intensities a detailed analysis of this spectral data is used to determine the identity and quantity of the radionuclides present in the sample.

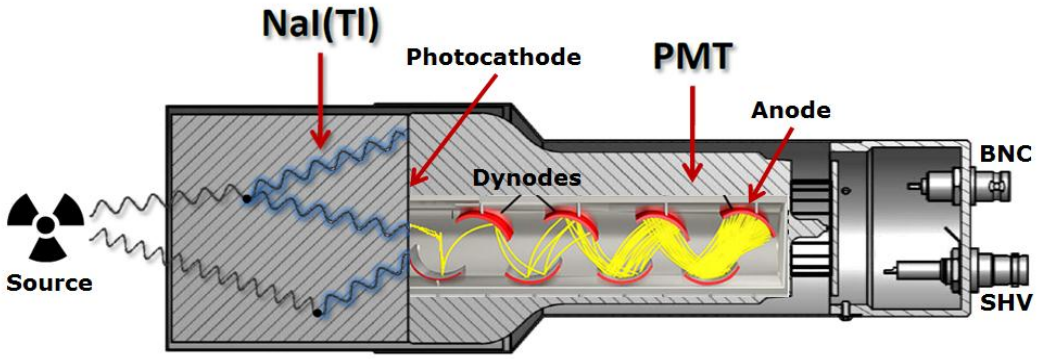

Fig 4.3: Schematic picture of the detector used in this work (Clark *et al*.1997).

4.5 Energy calibration of NAI (Tl) spectrometer

Energy calibration involved establishment of the channel number of the multichannel analyzer (MCA) in relation to gamma ray energy which was done using peaks of a source whose gamma ray energy and activity is known. ^{137}Cs and ^{60}Co was used for the calibration as a standard source. The gamma ray energy of any radionuclide spectra peak occurring within the calibrated area was read. The graph in figure 4.4 shows the spectrum displayed on the screen of the gamma ray spectrometer for ^{137}Cs and ^{60}Co.

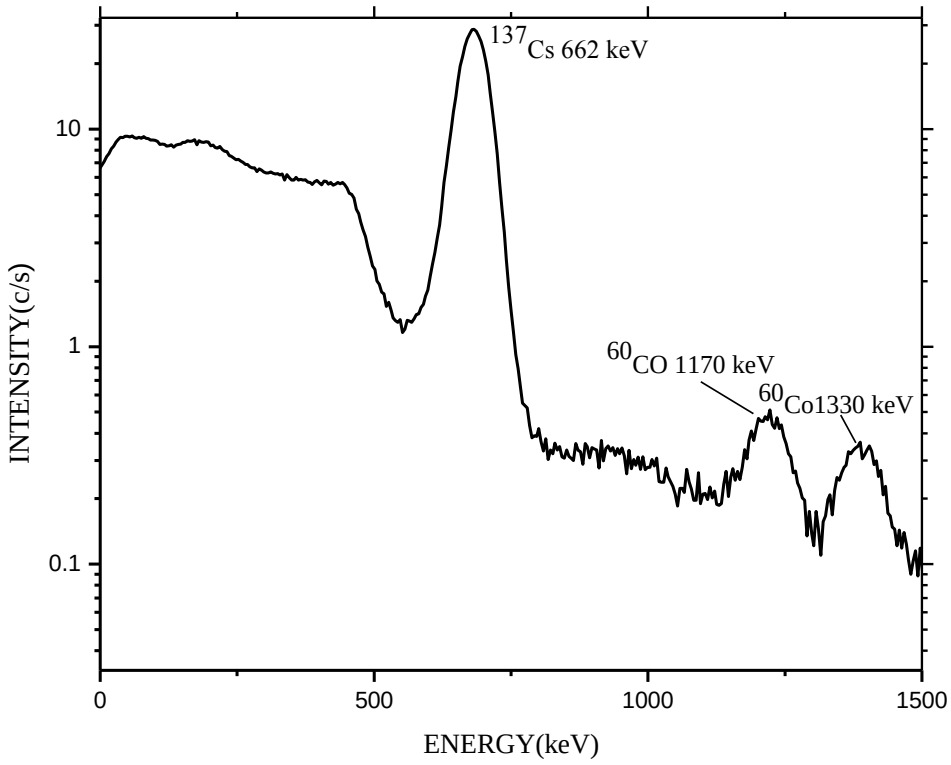

Fig 4.4: A typical gamma ray spectrum of ^{137}Cs and ^{60}Co.

The photo energy peaks of calibration are labeled in the graph in fig 4.3.To calibrate the spectrometer at the energy peaks of 662 keV, 1170keV and 1330

keV the energy as a function of the channel number was fit to a second order polynomial of the form given by equation 4.1.

$$E=E_O + B_1C + B_2C^2 \quad (4.1)$$

where:E_O,$B_1$and B_2 are constants and C is the channel number.

The graph in figure 4.5 shows a second order polynomial fit for energy as a function of channel numbers used for the energy calibration of the spectrometer used in this work.

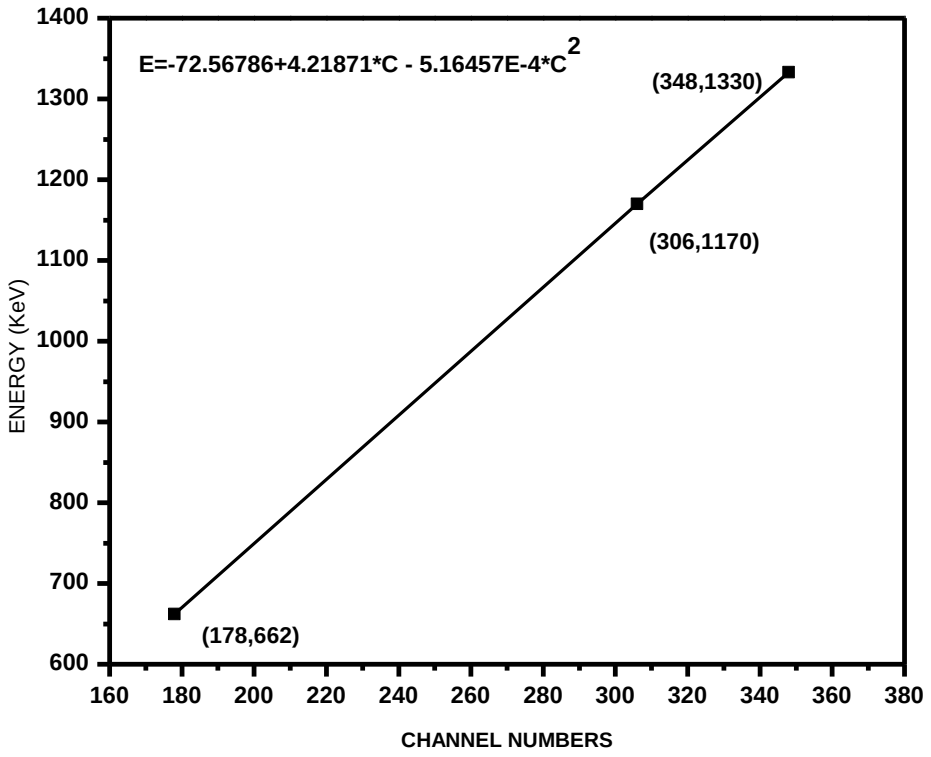

Fig 4.5: A second order polynomial fit for the calibration of NaI (Tl) detector.

The Table 4.1 Shows the fit parameters the for energy calibration of NaI (Tl) detector used in this work.

Table 4.1: Fit parameters in the second order polynomial.

Parameter	fit parameters(keV)
E_0	-72.6 ± 3.6
B_1	4.2 ± 0.2
B_2	-5.2E-4 ± 0.3

4.6 ENERGY RESOLUTION OF THE NaI (Tl) DETECTOR

A mono energetic point source of ^{137}Cs with a photo peak of 662 keV was used for energy resolution of the detector. It was obtained by fitting ^{137}Cs full energy peak at 662 keV to a Gaussian curve of the form in the equation shown in equation 4.2

$$y = y_0 + \frac{A}{W\sqrt{\pi}/2} e^{-\frac{(x-x_c)^2}{w^2}} \qquad (4.2)$$

The graph in figure 4.6 shows the Gaussian fit in which the energy resolution value of 7.81% ± 0.3 % was obtained for the NaI (Tl) detector used in this work.

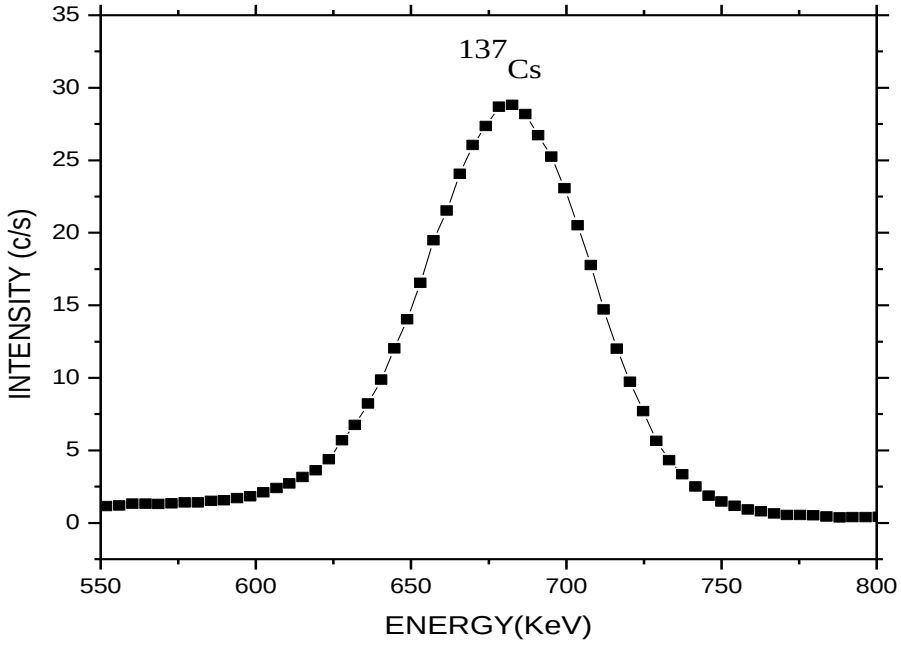

Fig 4.6: The energy spectrum of ^{137}Cs .

The solid line in the graph in fig 4.5 indicates a Gaussian fit for the measured Spectrum. The fit parameters for the determination of energy resolution are shown in Table 4.2

Table 4.2: Parameters obtained by the Gaussian fit of ^{137}Cs

Fit parameter	**Fitted value**
y_0 (offset)	0.33±0.03
X_c(peak position)	680.76 ± 0.98
W(peak width)	53.21±1.97
A(peak area)	613.46±19.87
X^2/Dof	0.64
R^2	0.59

Energy resolution = $\frac{FWHM}{EP} \times 100\%$ (4.3)

where:

FWHM (full wavelength at half maximum) = 53.21 $\pm$ 1.97 keV

EP (Energy at the peak) = 680.76 $\pm$ 0.98 keV

The energy resolution for the detector used was ≅7.82 $\pm$ 0.3%

4.7 Acquisition of data

Data acquisition time for each sample was approximately 3.0×10^4 seconds. The background spectrum was determined by using distilled water in a plastic container.

The spectrum of the background was used to determine the spectra components of the samples used. To obtain the net spectra of each sample the background was subtracted (Righi *et al*., 2009).

$Y_n = Y_t - Y_b$ (4.4)

where:

Y_n– is the net spectrum of the sample.

Y_t- is the total intensity

Y_b- is the background intensity

The graph in figure 4.7 Show the spectrum for background radiation intensity (c/s) against energy (keV).

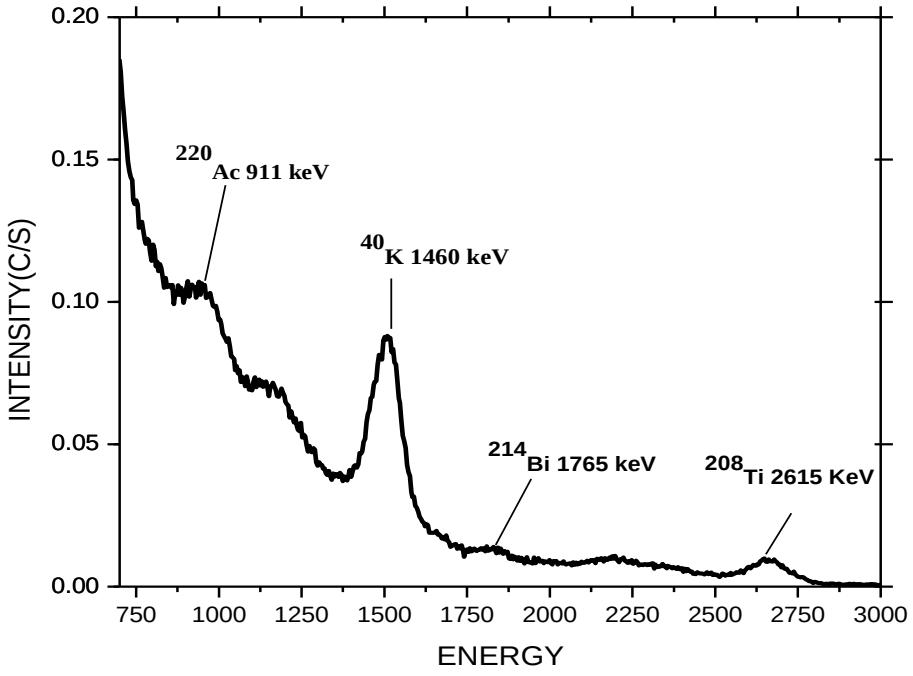

Fig 4.7: A gamma ray spectrum of background radiation.

4.8 Analysis of the samples

The radionuclides ^{238}U and ^{232}Th emit alpha particle and since the spectrometer cannot measure directly the activity concentration of these radionuclides, the activity concentration of the radioactive daughters ^{214}Bi (1765 keV) and ^{208}Tl (2615 keV) which are gamma emitters are used to measure activity concentration of these radionuclides respectively assuming secular equilibrium. The activity concentration of ^{40} K was measured using its 1460 keV gamma ray peak.

The graph in figure 4.8 shows a typical gamma ray spectrum for analyzed soil sample after background radiation is subtracted.

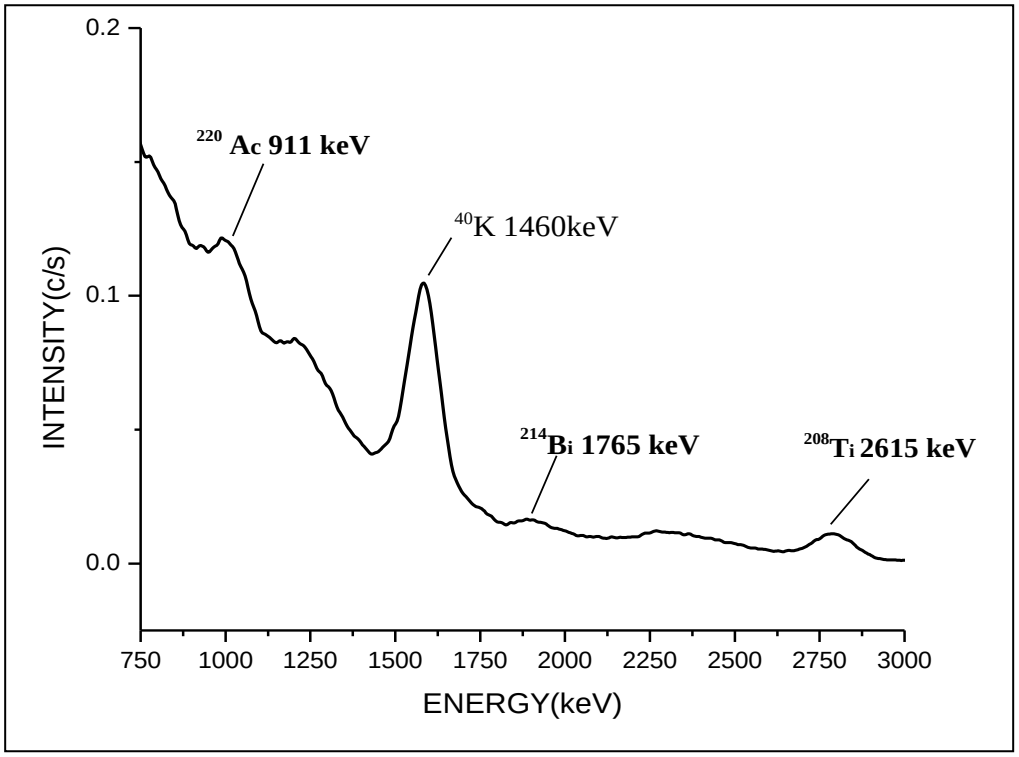

Fig 4.8: A typical gamma ray spectrum for analyzed soil sample after background subtraction

4.9 Calculation of radiological effects

4.9.1 Activity concentration

An IAEA approved reference sample RGMIX was used in determining the activity concentration of the samples collected. The following formula was used.

$$\frac{A_S M_S}{I_S} = \frac{A_R M_R}{I_R} \qquad (4.5)$$

where:

A_S- is the current activity of the specific radionuclide in the sample

M_S- is Mass of the sample in kilograms

I_S- is net count per second of the radionuclide in the sample

A_R- is current activity of the specific radionuclide in the reference sample

M_R –is mass of reference sample

I_R-Net count rate per second of the radionuclide in the reference sample

4.9.2 Absorbed gamma radiation dose rate (Ḋ)

This is the activity concentration in soil compared to the total absorbed dose rate in air at a unit height above the ground level (Abbady *et al.*, 2005).

$$\dot{D}=\sum A_{Ei}\ F_C \quad (4.6)$$

where

Ḋ - Is the dose rate

A_{Ei}-Activity concentration

F_c-Dose conversion factor

$$\text{DOSERATE } (\dot{D}) = 0.621A_{TH} + 0.462A_U + 0.0414A_K \quad (4.7)$$

where:

A_{Th} – Activity concentration of ^{232}Th

A_U - Activity concentration of ^{238}U

A_K is Activity concentration of ^{40}K while 0.621 nGyh^{-1},0.462 nGyh^{-1} and 0.0414 nGyh^{-1}are the conversion factors for^{232}Th,^{238}U&^{40}K respectively (Baranwal *et al*.,2006).

4.9.3 Effective dose rate (H_R)

The effective dose rate was calculated using the equation 4.8 (Turhan *et al.*, 2008)

$$H_R = \dot{D}TF_C \quad (4.8)$$

where:

H_R –Effective annual dose rate.

Ḋ – Absorbed dose rate

T - Out door occupancy time factor

F_C -Conversion factor, 0.7 $SvGy^{-1}$(UNSCEAR, 2000).

4.9.4 Risk assessment (G)

In order to estimate the number of people at risk from the sampled region a risk assessment index is calculated as follows.

$$G= F_C H_R P \quad (4.9)$$

where:

G -is the estimated number of deaths due to exposure to the ionizing radiations.

F_C-is dose to risk conversion factor, 5% per sievert (ICRP, 1991).

H_R -is effective annual dose rate

P –is the total population in the selected area .It gives an estimate of the number of people likely to die due to annual effective dose in a given population (Durham, 2007).

4.9.5 Radium equivalent activity (Ra_{eq})

This quantity compares the specific activities of materials containing ^{40}K, ^{238}U and ^{232} Th by a single quantity and which takes into account the radiation hazards associated with them (Avwiri *et al* .,2012)

$$Ra_{eq} = C_{Ra} + F_{Th}C_{Th} + F_K C_K \quad (4.10)$$

where:

$C_{Ra,}\ C_{Th}\ \ C_K$ are the activity concentrations of radium, thorium and potassium respectively while F_{Th} and F_K are conversion factors for thorium and potassium with F_{Th}=1.4286 and F_K=0.07692.

4.9.6 Internal hazard index (H_i)

This is due to the short lived radon which escapes through cracks in the houses. It is calculated as

$$H_i = \frac{A_{RA}}{185} + \frac{A_{TH}}{259} + \frac{A_K}{4810} \quad (4.11)$$

where:

A_{RA} – Is the radium activity

A_{TH}- Is the thorium activity

A_K –Is the potassium activity

4.9.7 External hazard index (H_e)

This hazard index is used to assess the radiological suitability of soil and rocks. It is calculated as follows

$$H_e = \frac{A_{RA}}{370} + \frac{A_{TH}}{259} + \frac{A_K}{4810} \quad (4.12)$$

where

A_{RA} – Is the radium activity

A_{TH} - Is the thorium activity

A_K–Is the potassium activity

4.9.8 Alpha index ($I_{\propto}$)

This index is used to assess the excess alpha radiation due to radon inhalation from soil and rocks. It's calculated as (Righi *et al.*, 2006):

$$I_{\propto} = \frac{A_{RA}}{200} \quad (4.13)$$

where

A_{Ra} – Is the radium activity

$I_{\propto}$ - is the alpha index

4.9.9 Representative level index (Ig)

This hazard index is used to access gamma radiation hazard associated with natural radioactivity calculated as (Abbady, 2005).

$$I_g = \frac{A_{Ra}}{150} + \frac{A_{TH}}{100} + \frac{A_K}{1500} \quad (4.14)$$

where, A_{Ra}, A_{TH} and A_K are the activity concentrations of ^{222}Ra ^{232}Th and ^{40}K respectively.

4.9.10 Quality assurance

For quality assurance the following steps were taken.

- Each sample was run in the detector three times and an average of the values calculated.
- All particles were of the same geometry in each sample.
- All samples were of the same mass.

CHAPTER FIVE

RESUTS AND DISCUSSION

The main objective of this study was to measure radioactivity concentration levels of naturally occurring radionuclides ^{238}U, ^{232}Th and ^{40}K from selected areas of Makueni County. The collected samples were prepared and analysis was done at the Kenyatta University Physics laboratory. The analysis measured activity concentration levels, absorbed gamma radiation dose rate, effective dose rate, risk assessment, radium equivalent activity, internal and external hazard indices, the alpha index and the representative level index. In this chapter all the results are given and discussion of the same done.

5.1 Activity concentration levels of natural radionuclides

(a) Soil samples

Activity concentration in soil of ^{238}U, ^{232}Th and ^{40}K was calculated and the result presented in table 5.1**.** The minimum activity of ^{238}U, ^{232}Th and ^{40}K observed are 35$\pm$6 Bq/Kg , 7$\pm$3 Bq/Kg, 690$\pm$79 Bq/Kg while the maximum values were 104 $\pm$3 Bq/Kg, 170$\pm$4 Bq/Kg and 1782$\pm$72Bq/Kg respectively, The average concentration was, 69$\pm$5Bq/Kg, 53$\pm$3Bq/Kg and 1098$\pm$69 Bq/Kg for ^{238}U, ^{232}Th, ^{40}K respectively. These values are above the world's average values of 33Bq/kg, 45Bq/kg and 420 Bq/kg for ^{238}U, ^{232}Th and ^{40}K respectively (UNSCEAR, 2000).

Table 5.1: Activity concentration of radionuclides in soil samples

SAMPLE	G.P.S LOCATION	^{238}U (Bq/Kg)	^{232}Th (Bq/Kg)	^{40}K (Bq/Kg)
NZS1	1.9661^{0}S ,37.4566^0 E	61 ± 4	7 ± 3	1323 ± 71
NZS2	2.1341^{0}S ,37.5879^0 E	37 ± 2	20 ± 1	788 ± 34
NZS3	1.9943^{0}S ,37.5380^0 E	47 ± 9	105 ± 2	691 ± 63
NZS4	1.9484^{0}S ,37.4706^0 E	139±4	21 ± 6	1782 ± 72
NZS5	1.9728^{0}S ,37.4651^0 E	92 ± 6	108 ± 3	904 ± 47
NZS6	2.1514^{0}S ,37.6499^0 E	35 ± 6	170 ± 4	784 ± 78
NZS7	2.0040^{0}S ,37.5625^0 E	58 ± 4	50 ± 4	690 ± 79
NZS8	1.9614^{0}S ,37.5689^0 E	69 ± 8	27 ± 3	1718 ± 76
NZS9	1.9112^{0}S ,37.5689^0 E	104±3	14 ± 2	911 ± 81
NZS10	2.0878^{0}S ,37.5465^0 E	47 ± 3	12 ±3	1385 ± 83
MEAN		**69 ± 5**	**53 ± 3**	**1098 ± 69**

The recorded high concentrations in soil is due to the presence of radioactive rich, Quartzite, the muscovite -schist ,Granite and the biotite gneisses which are eroded from the western hills in this county and spreads in the lowlands. It is noted that the activity concentration of ^{40}K is higher in this region than other parts of Kenya (Hashim *et al*., 2004). This is because there is use of fertilizers rich in potassium for farming especially during planting seasons. Sample NZS6 recorded the highest value of ^{232}Th concentration (170±4Bq/Kg) due to the presence of igneous rocks like the granitoid gneiss, the biotite gneisses and the feldspar in that area which over the years have undergone weathering to form the soil. This place is known as Masamukye in Nguu division, which in the local dialect means "*boiled* or *heated"* due to the presence of hot springs, the water is warm and put for domestic use. All samples gave high concentration of ^{40}K due to the presence of granite,

quartzite rocks and hornblende granulite which contain a high concentration of this radionuclides and have undergone weathering to form soil in that area.

Bar graph in figure 5.1 shows the activity concentration of all the soil samples.

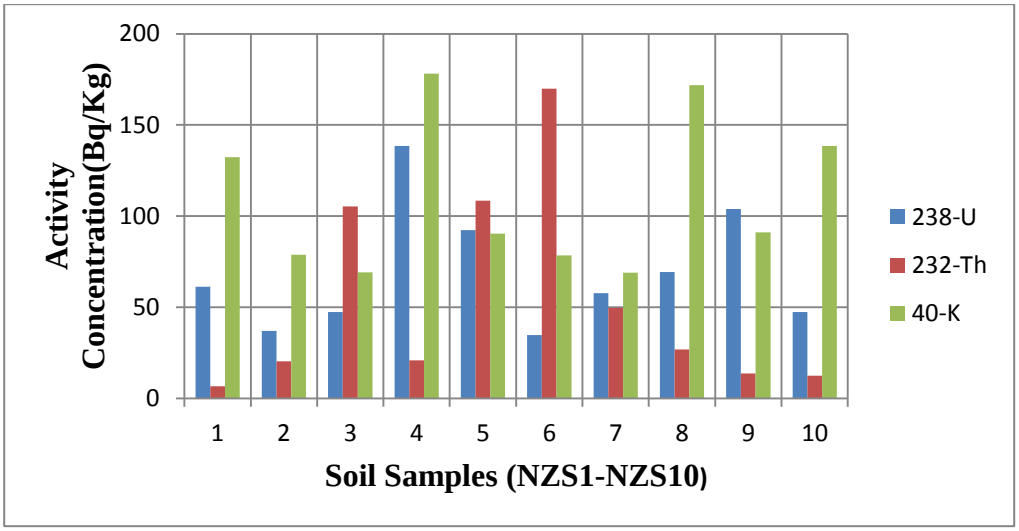

Fig 5.1: Activity concentrations of the natural radionuclides ^{238}U, ^{232} Th and ^{40}K in soil samples. The values for ^{40}K have been scaled down by a factor ten.

(b) Rock samples

Radioactivity concentration in rocks in this area is averagely higher than in the soil samples collected. Generally rocks contain higher radioactivity concentration than soil due to mixing of debris from weathered parent rock with organic materials (Yu *et al*., 1992). The minimum activity of ^{238}U,^{232}Th,^{40}K observed are 82 $\pm$ 3 Bq/Kg,10 $\pm$ 1 Bq/Kg and 698 $\pm$ 39 Bq/Kg while the maximum values are 208 $\pm$9 Bq/Kg,200 $\pm$3 Bq/Kg and 2200$\pm$75Bq/Kg. The average values are 139 $\pm$ 6 Bq/Kg, 73 $\pm$ 3 Bq/Kg and 1573 $\pm$ 65 Bq/Kg for ^{238}U, ^{232}Th and ^{40}K. The overall radioactivity concentration is higher in the igneous rocks than sedimentary rocks. The table 5.2 shows the activity concentration in rock samples analyzed.

Table 5.2: Activity concentration of radionuclides in rock samples

SAMPLE	G.P.S LOCATION	^{238}U(Bq/Kg)	^{232}Th(Bq/Kg)	^{40}K(Bq/Kg)
NZR1	2.0804^{0}S ,37.5467^{0}E	104 ± 2	10 ±1	1405±50
NZR2	2.0921^{0}S, 37.5740^{0}E	208 ± 6	29 ± 5	2032±36
NZR3	2.1508^{0}S ,37.6691^{0}E	92 ± 1	20 ± 2	1816±75
NZR4	1.92132^{0}S, 37.5001^{0}E	208 ± 9	102±2	2200±75
NZR5	2.0302^{0}S ,37.4621^{0}E	104 ± 3	40+2	1776±81
NZR6	1.9330^{0}S ,37.4659^{0}E	196 ± 9	174±2	913±84
NZR7	1.89684^{0}S, 37.5072^{0}E	91 ± 5	82±4	1946±85
NZR8	2.1031^{0}S ,37.5721^{0}E	162 ± 8	63±3	2161±78
NZR9	1.9744^{0}S ,37.4541^{0}E	139 ± 9	200±3	698±39
NZR10	2.1289^{0}S ,37.5668^{0}E	82 ± 6	13±3	786±47
MEAN		**139 ± 6**	**73 ± 3**	**1573 ± 65**

Bar graph in figure **5.2** shows the activity concentration of the three primordial radioactive elements in the rock samples analysed.

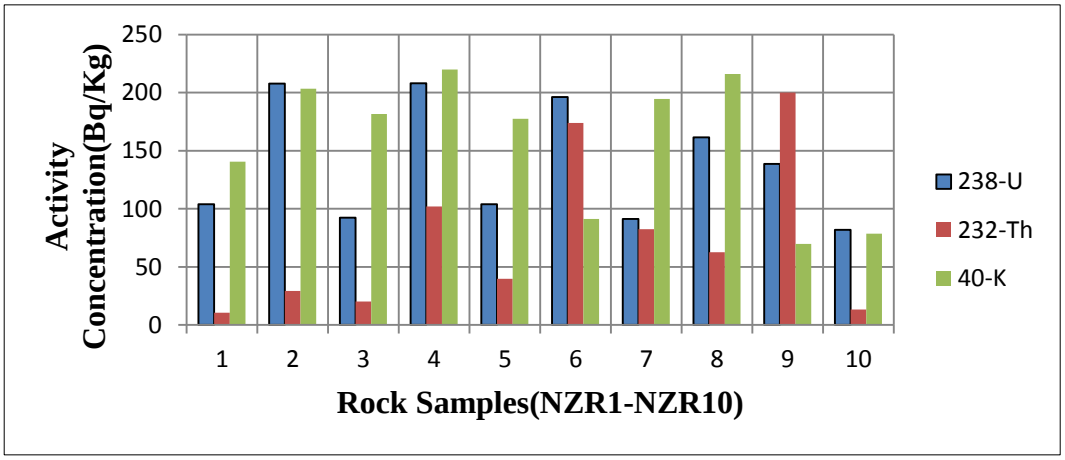

Fig 5.2: The activity concentration of the three primordial radioactive elements in the rock samples collected. The values for ^{40}K have been scaled down by a factor ten.

NZR4 is volcanic rock at Taiti area which is hilly in Kalamba Division. The common type of rock here is the intrusive amphibolite, the granite and the gneiss rocks all of which are igneous rocks and are rich in primordial radionuclides, sample NZR10 recorded the lowest value of ^{238}U due to the solubility of uranium as U^{6+} and therefore becomes mobile, this is metamorphosed sediments rocks from Nguu Division.

Sedimentary rocks have low radioactive concentration level due to the fact they are formed through compacting of plant and animal debris which contain low levels of radioactive elements.

The activity concentration of ^{238}U, ^{232}Th and ^{40}K in soil and rock samples were plotted in a graph in figure 5.3

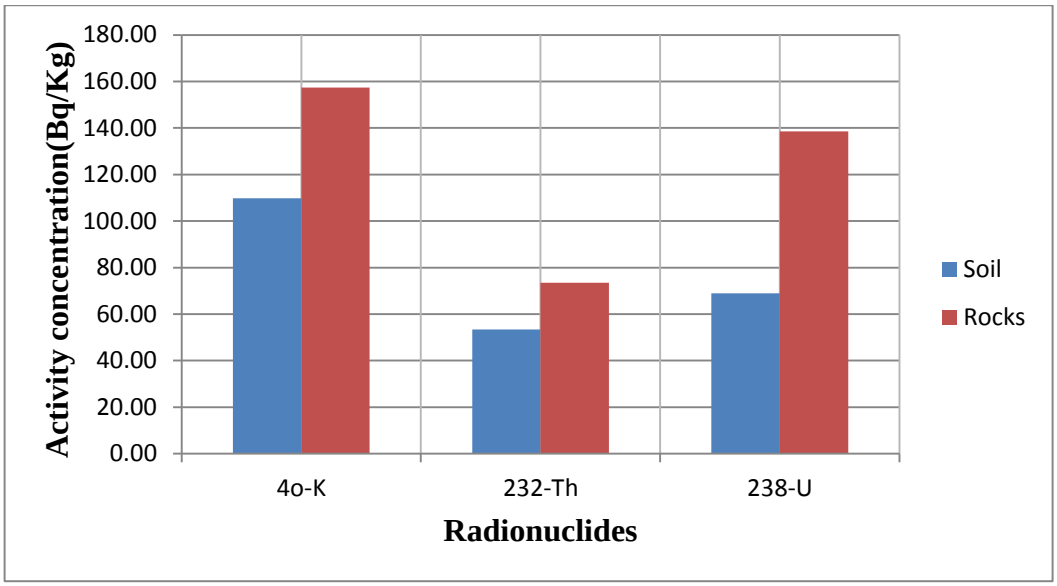

Fig 5.3: Average activity concentration of ^{238}U, ^{232}Th and ^{40}K in soil and rock samples. Values for ^{40}K have been scaled down by a factor of ten.

The concentration of ^{40}K is higher in rocks than in soils due to solubility of ^{40}K in soils. The average activity concentration of radionuclides in the samples collected in this region compared to the word average are shown in table 5.3

Table 5.3: Concentration of the radionuclides in both rocks and soils.

Radionuclide	**Radionuclide concentration** (Bq/Kg)	**World average** (UNSCEAR,2000)
^{40}K	1335.53 $\pm$ 66.78	420 Bq/Kg)
^{232}Th	63.41 $\pm$ 3.17	45 Bq/Kg)
^{238}U	103.72 $\pm$ 5.19	33 Bq/Kg)

The average concentration for both soils and rocks in this region is higher than the world averages. This region has the basement rocks like the granitoid gneiss around Nzaui hill (Kalamba division), The schistose biotite gneiss in Matha area (Matiliku division),the granite in Taiti area and the volcanic rocks in Emali (Mulala division) (GOK, Geology of Simba-Kibwezi area, 1963; GOK, Geology of South East Machakos Area,1954 Reprint,2007). These rocks contain high levels of the primordial radionuclides.

Soils in the lowland areas in Nguu division like Masamukye consist of red soil which is weathered from granite parent rock in the hills on the western part of this region which consist of Taiti hill in Kalamba Division and Kyemundu hill in Mbitini division. The soils erode spreading uniformly over the lowlands, with time, together with the application of phosphate and potassium fertilizers during irrigation of crops in rivers like Muooni and Kikuu, introduces radioactive elements in the soils and erodes during the rainy season to reach the lowlands.

This region has the highest concentration of ^{40}K compared to other researchers in other areas in Kenya. However ^{232}Th and ^{238}U concentration is lower than in Kibwezi District and Mrima Hill.

5.2 Absorbed gamma radiation dose rate (Ḋ)

The absorbed gamma radiation dose rate is a quantity which represents the mean energy imparted to matter both living and non-living per unit mass by an ionizing radiation .This is calculated at a unit height above the ground since most life exist averagely at that height (1m). It's calculated using the equation 4.7.

In rocks this value ranged from 79 $\pm$ 5 $nGyh^{-1}$ to a maximum of 251 $\pm$ 9 $nGyh^{-1}$ with an average of 175 $\pm$7 $nGyh^{-1}$ while in soil the value ranged from 62 $\pm$ 3 $nGyh^{-1}$ to a maximum value 154 $\pm$ 9 $nGyh^{-1}$ with an average value of 110 $\pm$ 7 $nGyh^{-1}$.The graph in figure 5.4 shows the graphical presentation of the calculated dose rates in rocks. The word average is 60 $nGyh^{-1}$ for both rocks and soil (UNSCEAR, 2000). Both these values from the analyzed samples are higher than the word average.

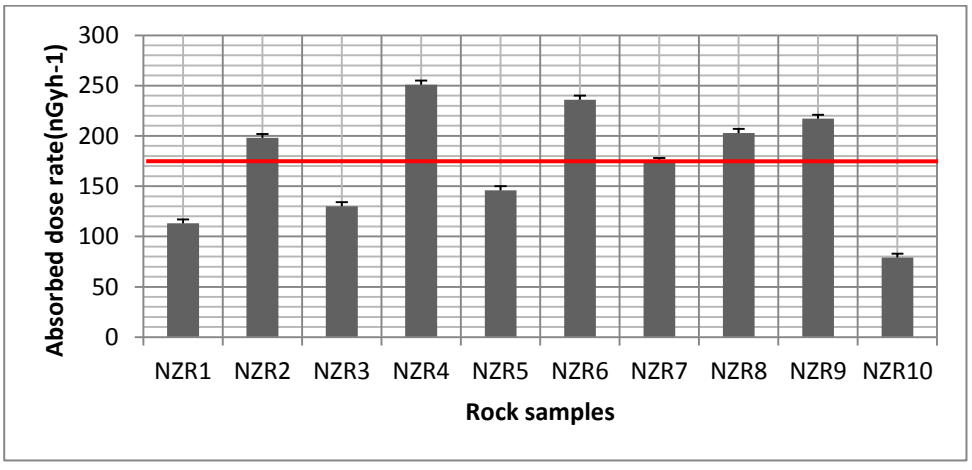

Fig 5.4: Absorbed gamma radiation dose rate in rock samples.

The red line shows the average value of 175 $\pm$ 7 $nGyh^{-1}$.World average is 60 $nGyh^{-1}$ (UNSCEAR, 2000)

The graph in figure 5.5 shows the absorbed dose rate in the analyzed soil samples.

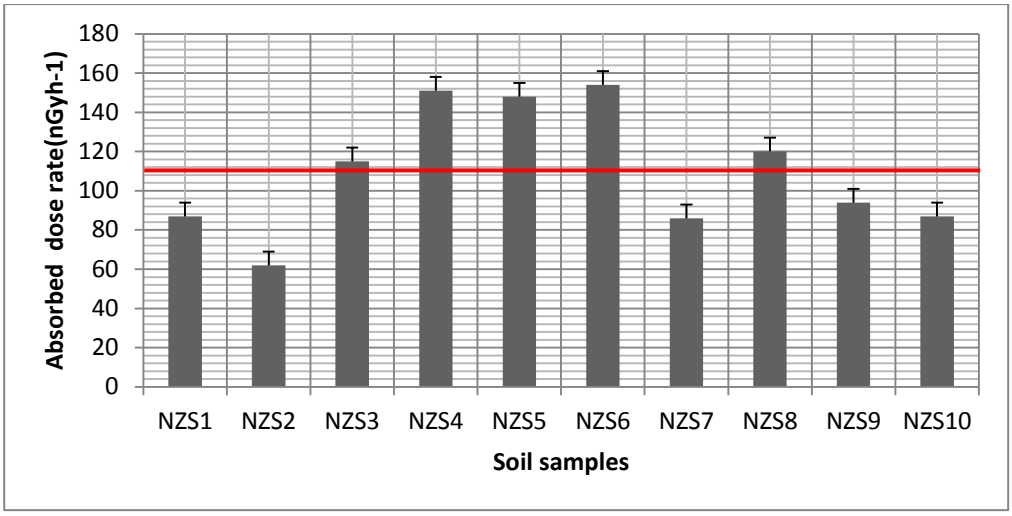

Fig 5.5: Absorbed gamma radiation dose rate in the soil samples.

The red line represents the average dose from soil in this area, 110 $\pm$ 7 $nGyh^{-1}$. In both rocks and soil samples the average value for absorbed gamma radiation dose is below maximum safe health limit of 1500 $nGyh^{-1}$ (UNSCEAR, 2000).

5.3 Effective dose per year (H_R)

The effective dose rate is a quantity which represents the risk of ionizing radiation to the whole body of an individual; it can also be taken as the probability of cancer induction and the genetic effects due to low level of ionizing radiations. It was calculated using the equation 4.8 In soil samples analyzed it ranged from 0.161 $\pm$ 0.01 $mSvy^{-1}$ to a maximum value of 0.398 $\pm$ 0.02 $mSvy^{-1}$ with an average of 0.29 $\pm$ 0.02 $mSvy^{-1}$. While in the rocks the range was 0.203 $\pm$ 0.02 $mSvy^{-1}$ to 0.647 $\pm$ 0.03 $mSvy^{-1}$ with an average of 0.45 $\pm$ 0.02 $mSvy^{-1}$. The graph in figure 5.6 shows the effective dose rate per year in the soil samples analyzed.

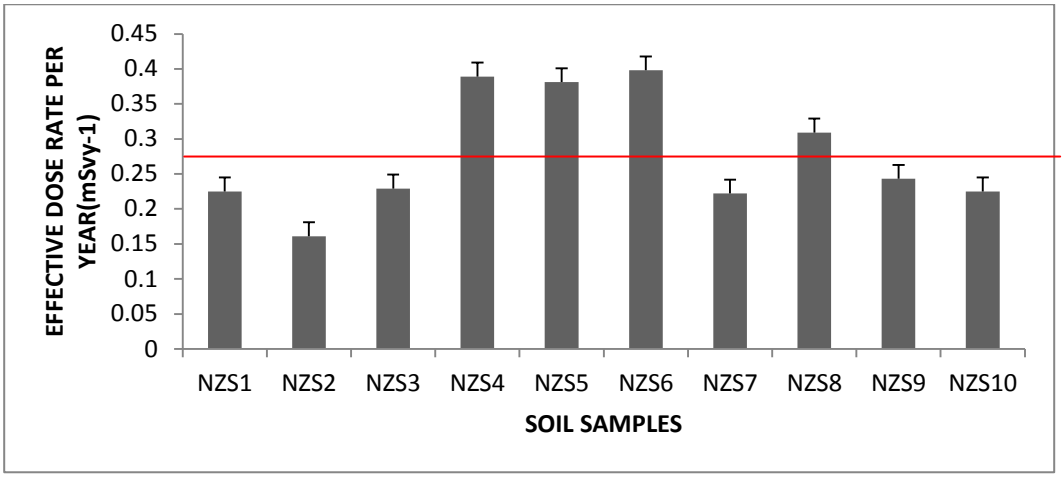

Fig 5.6: Effective dose rate per year in the soil samples.

The red line represents the average value in the soil samples analyzed 0.29 $\pm$ 0.02 $mSvy^{-1}$The graph in figure 5.7 shows the effective dose rate in rock samples analyzed.

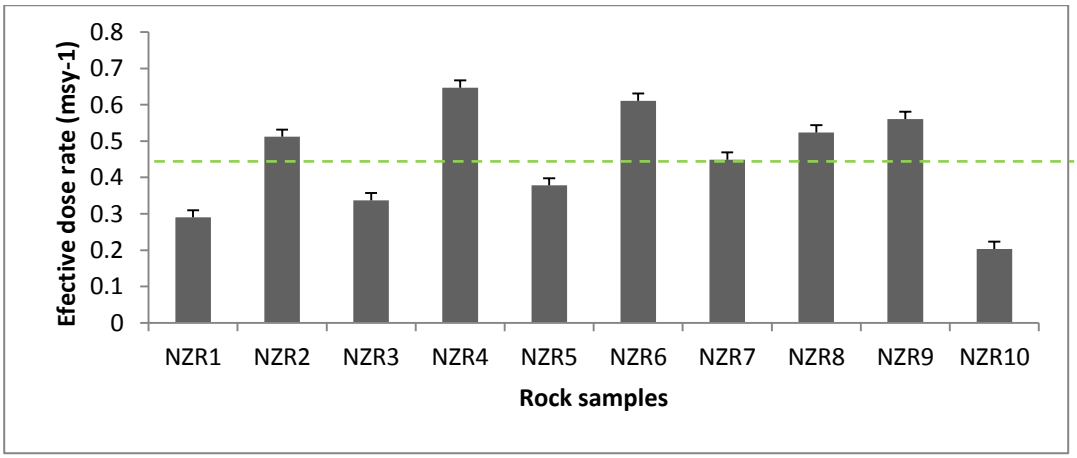

Fig 5.7: Effective dose rate in rocks.

The dotted line in the graph in Fig 5.7 represents the average effective dose in rock samples, 0.45 $\pm$ 0.02$mSvy^{-1}$.This is below the world average value of 0.48 $mSvy^{-1}$ (UNSCEAR, 2000) and also below the safe limit for members of the general public of 1$mSvy^{-1}$(ICRP, 1991).

5.4 Risk assessment (G)

This risk index estimates the number of people at risk from the ionizing radiations (Durham, 2007). The population of the select area (Former Nzaui district) is 204,675 people (GOK.The 2009 Kenya population and Housing Census Report pp. 93: Nzaui District). A dose to risk conversion factor (DCRF) of 5% per sievert (ICRP, 1991) has been applied to this population. The pie chart on fig 5.8 shows the people at risk in the population of the select region.

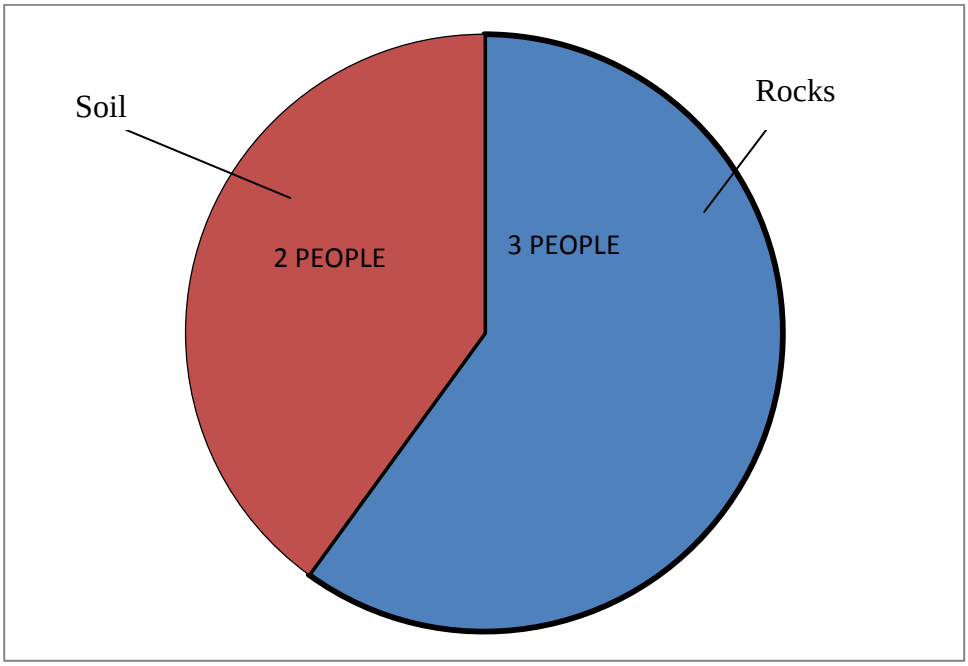

Fig 5.8: People at risk from the ionizing radiations.

From the graph in fig 5.8, people at risk from ionizing radiations in this population is three and two persons per year for rocks and soil respectively, However this depends on the type of radiation, the organ exposed to the ionizing radiation, the duration of exposure and the dose of radiation and therefore a constant monitoring and evaluation is necessary.

5.5 Radium equivalent activity (Ra_{eq})

This quantity compares the specific activities of materials containing ^{40}K, ^{238}U and ^{232} Th by a single quantity and which takes into account the radiation hazards associated with them (Avwiri *et al* .,2012). It is calculated using equation 4.10. For building materials from a particular place to be safe this value should be less or equal to 370 Bq/Kg (Avwiri *et al*., 2012, OECD 1979).In this research the value for rock samples analyzed ranged from 161.6 ± 10.98 Bq/Kg to 522.8 ± 17.92 Bq/Kg with an average of 364.44±14.7Bq/kg While for soil samples the range was 126.5 ± 6.6 Bq/kg to337.7±17.9 Bq/kg with an average of 229.69 ± 13.6 Bq/Kg.

The graph in figure 5.9 shows the radium equivalent activity in rock samples.

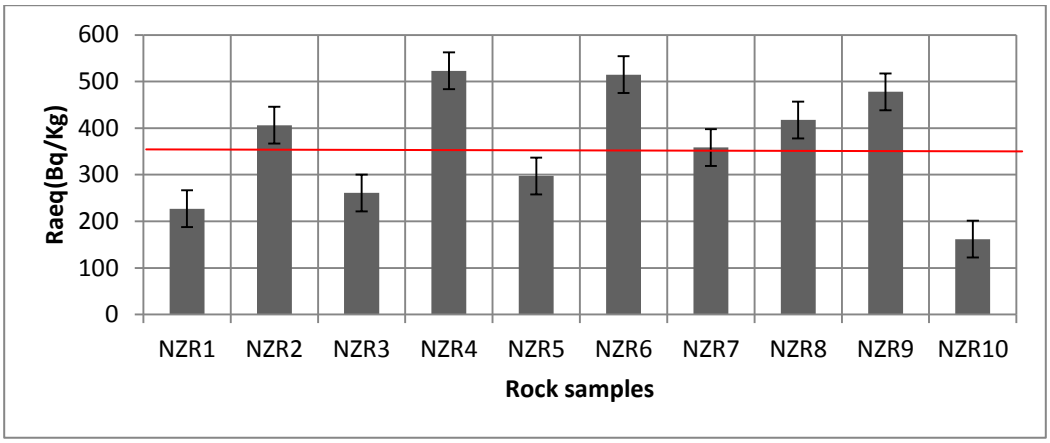

Fig 5.9: Radium equivalent activity (Ra_{eq}) in rock samples.

The red line in fig 5.9 shows the average radium activity in rocks, 364.44 ± 14.7 Bq/kg. In soil samples, Radium equivalent activity (Ra_{eq}) was lower than in rocks. The graph in figure 5.10 shows the radium equivalent activity in soil samples.

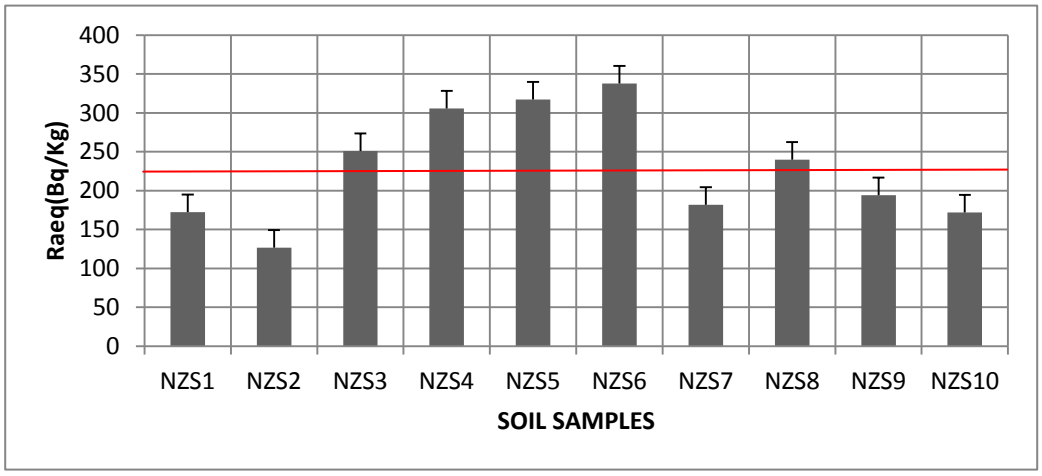

Fig 5.10: Radium equivalent activity in soil samples.

The red line in fig 5.10 represents the average value for radium equivalent activity in soil samples: 229.69 $\pm$13.6 Bq/Kg. The world average for radium equivalent activity is 89 Bq/Kg however for both soil and rock values in this region the average is below the maximum safe limit of 370 Bq/Kg (ICRP, 1991).

5.6 Hazard indices

In order to determine the radiological suitability of building material, radiological parameters were calculated, these are: Internal hazard index (H_i), external hazard index (H_e), alpha index (I_α) and the representative level index (I_g)**.**

The table 5.4 shows the values for these indices in rocks.

Table 5.4: Distribution of H_i , H_e $I_\propto$ and I_g in rock samples

Sample	G.P.S location	Internal hazard index(H_i)	External hazard index(H_e)	Alpha index ($I_\propto$)	Rep. level index (I_g)
NZR1	2.0804^0S ,37.5467^0E	0.89 ± 0.01	0.61 ± 0.02	0.52 ± 0.01	1.73 ± 0.03
NZR2	2.0921^0S ,37.5740^0E	1.66 ± 0.01	1.10 ± 0.05	1.04 ± 0.03	3.03 ± 0.05
NZR3	2.1508^0S ,37.6691^0E	0.95 ± 0.02	0.71 ± 0.03	0.46 ± 0.01	2.03 ± 0.01
NZR4	1.92132^0S ,37.5001^0E	1.98 ± 0.05	1.41 ± 0.05	1.04 ± 0.04	3.87 ± 0.03
NZR5	2.0302^0S ,37.4621^0E	1.92 ± 0.01	0.80 ± 0.03	0.52 ± 0.02	2.27 ± 0.07
NZR6	1.9330^0S ,37.4659^0E	1.91 ± 0.03	1.39 ± 0.05	0.98 ± 0.05	3.66 ± 0.08
NZR7	1.89684^0S ,37.5072^0E	1.21 ± 0.02	0.97 ± 0.05	0.46 ± 0.03	2.73 ± 0.06
NZR8	2.1031^0S ,37.5721^0E	1.56 ± 0.03	1.13 ± 0.05	0.71 ± 0.04	3.15 ± 0.05
NZR9	1.9744^0S ,37.4541^0E	1.67 ± 0.01	1.29 ± 0.04	0.69 ± 0.04	3.39 ± 0.01
NZR10	2.1289^0S ,37.5668^0E	0.66± 0.04	0.44 ± 0.03	0.41 ± 0.01	1.20 ± 0.03
MEAN		**1.44 ± 0.02**	**0.97 ± 0.04**	**0.68± 0.03**	**2.71 ± 0.04**

Internal hazard index H_i, originates from the short lived radon which escapes through small cracks in the house. It is hazardous to the respiratory system. For building materials to be safe for use this value should be less or equal 6. In this research, rock samples had a mean of 1.44 ± 0.02 Bq/Kg, while soil samples had mean of 0.90 ± 0.03 Bq/Kg.

Rock sample NZR4 recorded the highest value of internal hazard index; it's a sample from the Taiti hill in Kalamba division which was as a result of volcanicity. Most of the rocks are granite, the boitite gneiss and gabbro rich in

primordial radionuclides. Rock sample NZR5 is from Matiku in Mbitini Division, this area is rich in the igneous rocks which contain primordial radionuclides.

Soil sample NZS6 recorded the highest value of internal hazard index of 1.92 $\pm$ 0.04 since it's a olivine basalt rock, and the pyroxene these are volcanic rocks from Masamukye in Nguu division.

The radiological suitability of building materials is also tested by the external hazard index. In this study rocks had a mean of 0.97 $\pm$ 0.04, while soil had a mean of 0.62 $\pm$ 0.04, the recommended safe limit is 6.0 and the world average is 1.00

The excess alpha radiation due radon inhalation for both soil and rocks is estimated by the alpha index($I_{\propto}$).Rocks had a mean of 0.68 $\pm$ 0.03 Bq/Kg while the soil samples had a mean of 0.35 $\pm$ 0.03 Bq/Kg. The world average is 1 Bq/Kg while the accepted safe limit is 6 Bq/Kg.

To access gamma radiation hazard associated with natural radioactivity representative level index (I_g) is calculated. Rocks had an average of 2.71 $\pm$ 0.04 Bq/Kg while soil had a mean of 1.73 $\pm$ 0.05 Bq/Kg .It should be less than 6 for building materials to be safe. These values are within the safe limits.

The graph in figure 5.11 shows the distribution of H_i , H_e $I_{\propto}$ and I_g in rock samples.

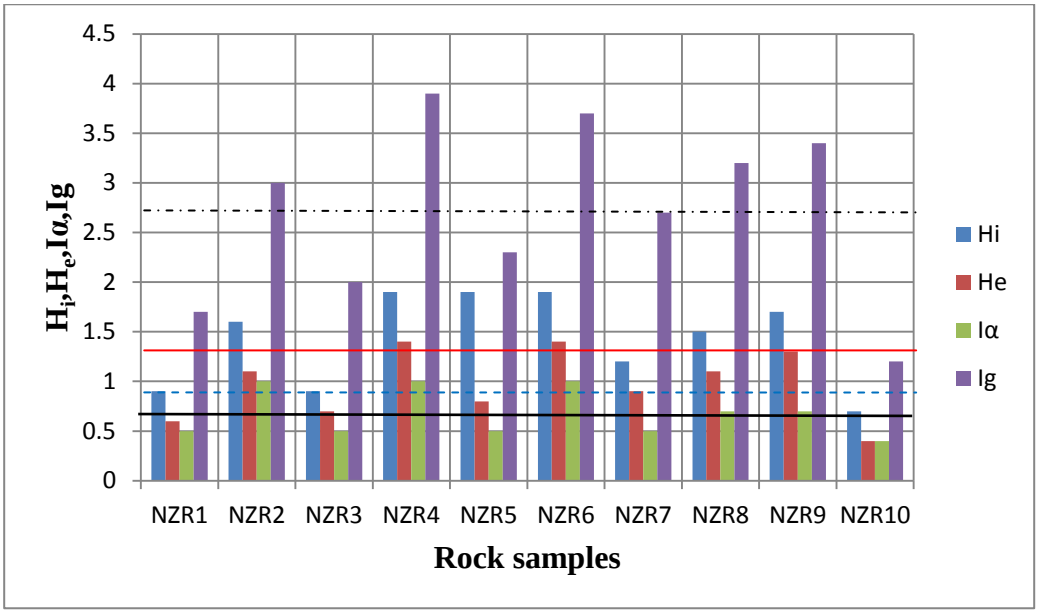

Fig 5.11: Distribution of H_i, H_e, I_α and I_g in rocks.

The red line shows the internal hazard index (1.44). The blue dashed line represents the external hazard index (0.97), the black solid line represents the alpha index (0.68) while the black dashed line represents the representative level index in rocks (2.71).

In soil samples the value are lower than in rock samples. The table 5.5 shows the calculated values of H_i, H_e, I_α and I_g in soil samples.

Table 5.5: Distribution of H_i, H_{ex} I_α and I_g in soil samples.

Sample	G.P.S LOCATION	Internal Hazard Index (H_i)	External Hazard Index(H_e)	Alpha Index ($I\alpha$)	Rep. Level Index(Ig)
NZS1	1.9661^0S ,37.4566^0E	0.63±0.01	0.47 ± 0.04	0.31 ± 0.02	1.36 ± 0.01
NZS2	2.1341^0S ,37.5879^0E	0.44±0.03	0.34 ± 0.02	0.18 ± 0.01	0.97± 0.03
NZS3	1.9943^0S ,37.5380^0E	0.81 ±0.02	0.68 ± 0.04	0.24 ± 0.05	1.83 ± 0.07
NZS4	1.9484^0S ,37.4706^0E	1.20 ±0.01	0.83 ± 0.05	0.69 ± 0.02	2.32 ± 0.05
NZS5	1.9728^0S,37.4651^0E	1.11 ±0.03	0.86 ± 0.04	0.46 ± 0.03	2.30 ± 0.02
NZS6	2.1514^0S,37.6499^0E	1.92 ±0.04	0.91 ± 0.05	0.17 ± 0.03	2.45 ± 0.03
NZS7	2.0040^0S,37.5625^0E	0.65 ±0.01	0.49 ± 0.04	0.29 ± 0.02	1.34 ± 0.01
NZS8	1.9614^0S,37.4807^0E	0.84 ±0.02	0.65 ± 0.05	0.35 ± 0.04	1.88 ± 0.09
NZS9	1.9112^0S,37.5689^0E	0.81 ±0.03	0.52 ± 0.05	0.52 ± 0.02	1.44 ± 0.08
NZS10	2.0878^0S ,37.5465^0E	0.59 ±0.06	0.46 ± 0.04	0.24 ± 0.02	1.36 ± 0.07
MEAN		**0.90 ± 0.03**	**0.62 ± 0.04**	**0.35± 0.03**	**1.73±0.05**

Generally hazard indices in soils are lower than in rocks. This is because soils are as result of the weathering of the Parent rock. The graph in figure 5.12 shows the hazard indices in soil.

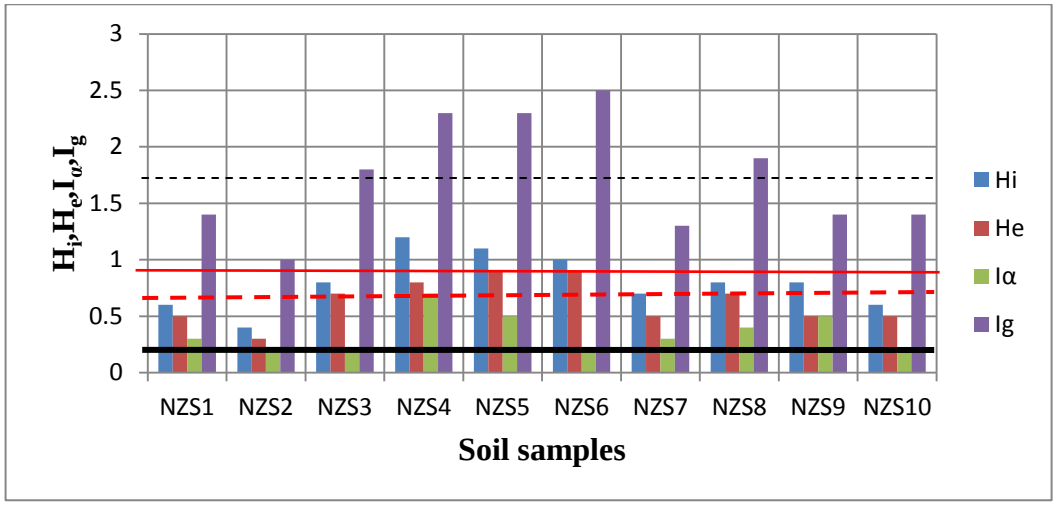

Fig 5.12: Distribution of H_i, H_{ex} I_α and I_g in soil samples.

The red solid line represents the average for internal hazard index (0.90), the red dotted line represents average for external hazard index (0.62), the black solid line represents the average for the alpha index (0.35) and the black dotted line represents the representative level index (1.73). The table 5.6 shows the recommended safe health limit for the hazard indices.

Table 5.6: Recommended safe health limit.

Hazard Index	Recommended safe health limit
H_R ($mSvy^{-1}$)	1 (ICRP,2007)
$D(nGyh^{-1})$	1500 (UNSCEAR ,2000)
H_i	6 (European Commission ,1999)
H_e	6 (European Commission ,1999)
I_g	6 (European Commission ,1999)
Raeq(Bq/Kg)	370 (ICRP,1991)

Comparing this safety limits to the values obtained from the samples collected from the selected areas in Makueni County it is observed that rocks and soil from this region are safe for use as building materials.

CHAPTER SIX

CONCLUSIONS AND RECOMENDATIONS

6.1 Conclusions

This study assessed the radioactivity concentration of soil and rock samples from selected areas of Makueni County using gamma ray spectrometric analysis. The activity concentration of ^{238}U, ^{232}Th and ^{40}K for rock samples showed an average concentration of 139 $\pm$ 6 Bq/Kg , 73 $\pm$3 Bq/Kg and 1573 $\pm$ 65 Bq/Kg. While for the soil samples the average activity concentration of ^{238}U, ^{232}Th and ^{40}K was 69 $\pm$ 5 Bq/Kg, 53 $\pm$ 3 Bq/Kg and 1098 $\pm$ 69 Bq/Kg respectively.

These values are higher than those reported in some high background areas as reported as 480 $\pm$ 24 Bq/Kg for ^{40} K and 26 $\pm$ 2 Bq/Kg for ^{232}Th and 23 $\pm$ 2 Bq/Kg for ^{238}U (Hashim *et al* .,2004). However the concentration of ^{232}Th is lower than the concentration of the same in high background region reported as 501 $\pm$ 20 Bq/Kg (Kebwaro., 2009) The activity concentration in this region is higher than the global average of 33 Bq/K , 45 Bq/Kg and 420 Bq/Kg for ^{238}U,^{232} Th and ^{40}K respectively.

Activity concentration in the selected areas of Makueni county is higher than the world average due to existence of igneous rocks like the granite, the pyroxene, the olivine basalt the migmatites and gabbro, the metamorphic rock like The quartzite and gneiss in various localities within the select area, this rocks contain higher radionuclide concentration than the metamorphosed rocks of sedimentary origin.

Natural processes like wind erosion during dry spells of February- March and August-October distribute the primordial radionuclides into the lowlands. During the rainy season, any remaining radionuclide is washed away and distributed by the rivers which pass through these hills. Muooni River has tributaries that

flow through Kyemundu hills in Mbitini division and through Emali hill, to cut through Nguu Division. This river deposits the radionuclides along its banks and they are taken from the main channel through irrigation processes along the river and distributed to the mainland. Kikuu river passes through Kalamba Division and has tributaries that pass through Taiti hill ,this river distribute the radionuclides down the stream. Rocks from Taiti hill, Kyemundu hill and the Nzaui hill have high concentration of radionuclides and undergo weathering to become soil which is distributed evenly across the region hence the high concentration of the radionuclides.

Effective dose rate in soil samples showed an average of 0.29 $\pm$ 0.02 $mSvy^{-1}$ while rocks showed an average of 0.45 $\pm$ 0.02 $mSvy^{-1}$,these values are below the world average of 0.48 $mSvy^{-1}$ (UNSCEAR,2000) and below the recommended limit for members of the public of 1 $mSvy^{-1}$ (ICRP 1991;UNSCEAR ,2002).The absorbed gamma radiation dose rate for samples of rocks was found to have an average of 175 $\pm$ 7 $nGyh^{-1}$ while the soil samples had an average of 110$\pm$7 $nGyh^{-1}$. These mean values are higher than the world average of 60$nGyh^{-1}$ (UNSCEAR, 2008), but below the recommended hazard limit of 1500 $nGyh^{-1}$, (UNSCEAR, 2000).

The hazard indices were calculated, in rocks external and internal hazard indices were found to be 0.97 $\pm$ 0.04 and 1.44 $\pm$ 0.02 while soils were found to be 0.62 $\pm$ 0.04 and 0.90 $\pm$ 0.02 both these values are less than the safe limit of 6 (European commission, 1999)The alpha index and the representative level index were found to be 0.68 $\pm$ 0.03 and 2.71$\pm$ 0.1 for rock samples and 0.35 $\pm$ 0.03 and 1.73 $\pm$ 0.05 for soil samples Both of the values were found to be below the recommended safe limits of 6 (European commission., 1999) and therefore this indicates that the radiation hazards from the selected areas of Makueni County (Kalamba, Matiliku, Mbitini, Mulala & Nguu divisions) is insignificant and the building materials are safe for use by members of the public.

6.2 Recommendations

The concentration level of ^{238}U in this region was 103.72 $\pm$ 5.19 Bq/Kg. This is higher than some regions in Kenya but less than the concentration of uranium in high background areas like Mrima hill 207.03 $\pm$ 11.3 Bq/Kg hence it's important to study the biological health impact to the inhabitants of this region arising from the gaseous randon inhalation associated with the availability of ^{238}U.

There is a possibility of radon build up in houses in this region; I recommend that the in habitants of this region build houses that are well ventilated for proper gaseous exchange.

This study involved soil and rock samples, I recommend for a similar study in plants and water samples from this region.

I recommend that the Government and non- governmental organizations use this study as a baseline study in radioactivity concentration levels of the area.

REFERENCES

Abbady, A. G. E., Uosif, M. A. and EL-Taher, A. (2005). Natural radioactivity and dose assessment for phosphate rocks from Wadi El-Mashal and El-Mahamidi mines in Egypt. *Journal of environmental radioactivity.* **84**: 65-78

Ademola, J. A. and Olatuji M. A. (2013). Evaluation of NORM and Dose Assessment in an Aluminum Industry in Nigeria. *World journal of nuclear science and technology.* **3**: 150-154.

Al-Jundi, J., Al-Bataina, B. A., Abu-Rukah, Y. and Shehadeh H.M. (2003). Natural radioactivity concentration in soil samples along the Amman Aqaba highway, Jordan. *Journal on radiation measurement*. **36**: 555-560.

Andrew, H.S. and Len, A. (1994). Handbook of radiation effects. New York. PP 37-41, 63, 299-300, 310.

Avwiri, G.O., Osimbi, J. C. and Agbalagba, E. O. (2012). Evaluation of radiation hazard indices and excess lifetime cancer risk due to natural radioactivity in soil profile of Udi and Ezeagu Local Government Areas of Enugu State, Nigeria. *Comprehensive journal of environmental and earth sciences*. **1**: pp1-10

Banzi, F. P., Kifanga, L. D. and Bundala, F. M. (2000). Natural radioactivity and radiation exposure at Minjingu phosphate mines in Tanzania. *A Journal on radiation protection*. Imprint of Elsevier. **20**: 41-51.

Baranwal, V. C., Sharma, S.P., Sengupta, D., Sandilya, M.K., Bhaumik, B.K., Guin, R. and Saha, S.K. (2006). A new background radiation area in the Geothermal Eastern Ghats Mobile Belt Of Orisa. *A journal on Indian Radiation Measurement*. **41**:602-610.

Bereznskii, V. S., Bulanov, S.V., Dogiel, V. A., Ginzburg, V. L. (Editor) and Sptusk, V. North Holland, (1990). Astrophysics of cosmic rays. pp. 72, 220-227.

Chege, M. W. (2007). Screening measurements of indoor radon-222 concentration by γ-ray spectrometry. Msc (Physics), Kenyatta University.

Chozzi, P., De felice, P., Fazio, A., Pasqual, V. and Verdayo, M. (2000). Laboratory application of NaI (TI) gamma ray spectroscopy to studies of natural radioactivity in Geophysics. *Journal of applied radiation and isotopes*. **53**:127-132.

Clark, R. B., Frid, C. and Atrill, M**. (**1997). Marine Pollution **(**4^{TH} EDITION**),** Oxford University Press, New york, USA.

Durham, J. (2007). Concepts, quantities and dose limits in radiation protection dosimetry radiation measurements. *A journal on radiation physics.* **41**: 28-35

European Commission, (1999). Radiological protection principles concerning the natural radioactivity of building materials. European Commission publication 112, (1999).

Gordon, R. G. (2008). Practical Gamma ray Spectroscopy. John Wiley and sons' limited. pp 25-38.

G.O.K, (2017). Kenya National Cancer Control Strategy, 2017-2022. Ministry of health report.

G.O.K, (1963). Geology of the Simba–Kibwezi Area, Report no 58. Geological Survey of Kenya.

G.O.K, (2009). Map of Nzaui District. Survey of Kenya, Nairobi, 2009.

Government of Makueni County, (2016). Makueni County Gazette supplement issue 20. Acts no 6. Government printer, Nairobi, (2016).

G.O.K, (1953, Reprint 2007). Geology of the South-East Machakos area Kenya. Report number 25. Geological Survey of Kenya.

G.O.K, (2010). The 2009 Kenya Population and Housing Census. Kenya National Bureau Of Statistics Report, 2010. Nairobi, Kenya.

Grupen, C. (2005). Astroparticle physics. Berlin Heidelberg. Germany

Hashim, N. O. (2001). The level of radionuclides and elements in selected Kenyan coastal ecosystems.Msc thesis (physics), Kenyatta University. Nairobi.

Hashim, N. O., Rathore, I.V.S., Kinyua, A. M. and Mustapha, A. O. (2004). Natural and artificial radioactivity in sediments along the Kenyan coast. *A journal on radiation physics and chemistry*.**71**: 805-806

Harb, S., El-Kamel, A., Abd El-Mageed A., Abbady A. and Negm, H. (2008). Natural radioactivity in soil and phosphate samples from El- Sabaea, Aswan, Egypt. *Journal on Radiation Physics, 15-19.* Nasr City-Cairo. Egypt.

Hayakawa, S. (1969). Cosmic ray physics, Vol XXII, pp. 109-113,422.

IAEA, (2004). Internal Atomic Energy Agency, Soil sampling for environmental contaminants. IAEA, Vienna, Austria.

IAEA, (2005). Radiation Oncology Physics: A handbook for Teachers and students. Internal Atomic Energy Agency, Vienna, Austria

ICRP, (1991). Annual limits on intake of radionuclides by workers based on1990 recommendations. International commission of radiological protection .Publication 61 annals of ICRP. **21:** 4.

ICRP, (2007). Recommendations of the International commission on radiological protection. Publication 103, (2007).

Internal Plant Nutrition Institute, (2008). Plant Nutrition article. Winter, 2008-2009. Georgia U.S.A.

Joshua, E. O., Ademola, J. A., Apanowo, M. A. and Olorode, D.O. (2009). Natural radionuclides and hazards of rocks samples collected from south eastern Nigeria. *Journal of radiation measurements*. **44**: 401- 404.

Kebwaro, M. J. (2009). Gamma spectrometric analysis of the service soils around Mrima hills, Kenya using NaI (TI) detector and decomposition techniques. Msc thesis (physics), Kenyatta University. Nairobi.

Langat, K. W. (2009). Gamma ray spectrometric analysis of sediments deposits at the shores of Lake Nakuru, Kenya. Msc thesis (Physics), Kenyatta University. Nairobi.

Merrie, E. and Thomas, G. (1997). Environmental radioactivity for natural, industrial and military sources, fourth edition. Academic press an imprint of Elsevier. 162-210.

Mohanty, A. K. S. D., Vijan, S. K. and Saha, S. K. (2004). Natural radioactivity in the newly discovered high background radiation area on the eastern coast of Orissa, India. *Radiation measurements*. **38**: 153-165.

Mutie, M. M. (2011). Measurement of the elemental and radionuclide concentrations of environmental and geological samples from selected areas of Kibwezi district, Kenya. Msc thesis (physics), Kenyatta University. Nairobi.

Osoro, K. M. (2007). Assessment of levels of natural radioactivity in surface soils around titanium mines in Kenya. Msc Thesis (physics), Kenyatta University. Nairobi.

O.E.C.D, (1979). Exposure to radiation from the natural radioactivity in building materials. Organization for Economic Co-Operation and Development Report, 1979.

Rhigi, S., Veerita, S., Albertazzi, A., Rossi, P.I. and Bruzz, I. (2009). Natural radioactivity in refractory manufacturing plants and exposure of workers to ionizing radiation. *Journal of environmental radioactivity*. **160**: 540-546**.**

Saad, H. R. and Al-Azmi, D. (2002). Radioactivity concentrations in sediments and their correlation to the coastal structure in Kuwait. *Journal on applied radiation isotope.* **56**: 991-997.

Santawamaitre, T. (2012). An evaluation of the level of naturally occurring radionuclide materials in soil samples along the Chao Phraya river basin. Ph.D. thesis, (physics). University Of Surrey, 2012.

Shenber, M.A. (1996). Measurement of natural radioactivity levels in soil in Tripoli. *A journal on applied radiation*. **48**: pp147-148.

Termizi, A. R., Wahab, A., Hussein, M. A. and Khalik, W. A. (2005). Environmental ^{238}U and ^{232}Th concentration measurement in area of high level natural background radiation at Palog Johor, Malysia. *Journal of environmental radioactivity*. **80**:287-304

Turhan, S., Baycan, U. N. and Sen, K. (2008). Measurement of natural radioactivity in building materials used in Ankara and assessment of external doses. *Journal of radiological protection*. **28**:83-91

Trevor, E., John, N. A. and Daniel, M. B. (2014). Dissolved Uranium, Radium and Radon evolution in the continental intercalaire (cl) aquifer, Algeria and Tunisia. *A journal on natural radioactivity*. An imprint of Elsevier. **137**:150-162.

UNSCEAR, (1993). Sources of Ionizing Radiations. United Nations Scientific Committee on Effects of Atomic Radiation, (UNSCEAR). 1993 report, United Nations, New York.

UNSCEAR, (2000). Sources of ionizing radiation. United Nations Scientific Committee on Effects of Atomic Radiation, (UNSCEAR). 2000 report, United Nations, New York.

UNSCEAR, (2002). Effects of Atomic Radiation United Nations Scientific Committee on Effects of Atomic Radiation, (UNSCEAR). 2002 report, United Nations, New York.

United Kingdom Government, (2016). Cancers due to ionizing radiations report. A report presented by the secretary of state for work and pensions by command of her majesty, February, 2016.

W.H.O, (2012). World Health Organization. Ionizing radiation in our environment. www.who.int/ionizing radiation/env/en. (Accessed on 28/10/2018).

Yu, K. N., Guan, Z. J., Stokes, M. J., Young, E. C. M. (1992). The assessment of the natural dose committed to the Hong Kong people. *Journal of Environmental Radioactivity*: 31-48

APPENDIX 1

Table A1: Human exposures to natural and artificial sources. (Clark *et al.,* 1997, WHO., 2012)

SOURCE	PERCENTAGE
Randon(Gas)	33.47%
Terrestrial	15.91%
cosmic sources	12.90%
others	1.20%
medical(x rays and others)	20.90%
internal activities	15.40%

APPENDIX 2

Table A2: Half-life of primordial radionuclides (Radiation Information Network, 2004)

RADIONUCLIDE	**HALF LIFE**
^{40}K	1.28×10^{9} years
^{232}Th	1.41×10^{10} years
^{238}U	4.42×10^{9} years

Table A3: Cosmogenic radionuclides with their half-life (Radiation Information Network, 2004).

RADIONUCLIDE	**HALF LIFE**
^{7}Be	53.3 days
^{3}H	12.3 years
^{14}C	5730 years

Table A4: Manmade radionuclides and their half-life.

RADIONUCLIDE	**HALF LIFE**
^{137}Cs	30 years
^{90}Sr	29.12 years
^{3}H	12.35 years

APPENDIX 3

TABLE A5**:** Absorbed dose rate in rocks.

SAMPLE	**ABSORBED DOSE RATE(D)($nGyh^{-1}$)**
NZR1	113 ± 4
NZR2	198 ± 8
NZR3	130 ± 5
NZR4	251 ± 9
NZR5	146 ± 6
NZR6	236 ± 9
NZR7	174 ± 9
NZR8	203 ± 9
NZR9	217 ± 8
NZR10	79 ± 5
AVERAGE	**175 ± 7**

APPENDIX 4

TABLE A6**:** Absorbed dose rate in soils.

SAMPLE	**ABSORBED DOSE RATE($\dot{D}$) ($nGyh^{-1}$)**
NZS1	87 $\pm$ 7
NZS2	62 $\pm$ 3
NZS3	115 $\pm$ 8
NZS4	151 $\pm$ 9
NZS5	148 $\pm$ 6
NZS6	154 $\pm$ 9
NZS7	86 $\pm$ 7
NZS8	120 $\pm$ 8
NZS9	94 $\pm$ 6
NZS10	87 $\pm$ 7
AVERAGE	110 $\pm$ 7

APPENDIX 5

TABLE A7 **:** Effective dose rate in soils.

SAMPLE	**Effective dose rate due to gamma radiation per year{mSvy^{-1}}**
NZS1	**0.225 ± 0.02**
NZS2	**0.161 ± 0.01**
NZS3	**0.229 ± 0.02**
NZS4	**0.389 ± 0.02**
NZS5	**0.381 ± 0.02**
NZS6	**0.398 ± 0.02**
NZS7	**0.222 ± 0.02**
NZS8	**0.309 ± 0.02**
NZS9	**0.243 ± 0.02**
NZS10	**0.225 ± 0.02**

APPENDIX 6

TABLE A8**:** Effective dose rate in rocks.

SAMPLE	**Effective dose rate due to gamma radiation per year{mSvy^{-1}}**
NZR1	0.291 $\pm$ 0.01
NZR2	0.512 $\pm$ 0.02
NZR3	0.337 $\pm$ 0.01
NZR4	0.647 $\pm$ 0.03
NZR5	0.378 $\pm$ 0.03
NZR6	0.611 $\pm$ 0.02
NZR7	0.449 $\pm$ 0.02
NZR8	0.524 $\pm$ 0.02
NZR9	0.561 $\pm$ 0.02
NZR10	0.203 $\pm$ 0.02

APPENDIX 7

TABLE A9**:** Radium equivalent activity in rocks.

SAMPLE	**RADIUM EQUIVALENT ACTIVITY (Bq/Kg)**
NZR1	226.9 ± 7.59
NZR2	406.1 ± 16.67
NZR3	261.0 ± 9.62
NZR4	522.8 ± 17.92
NZR5	297.4 ± 12.05
NZR6	514.8 ± 19.03
NZR7	358.5 ± 17.73
NZR8	417.4 ± 18.58
NZR9	477.9 ± 16.41
NZR10	161.6 ± 10.98

APPENDIX 8

TABLE A10**:** Radium equivalent activity in soils.

SAMPLE	**RADIUM EQUIVALENT ACTIVITY Bq/Kg**
NZS1	172.3 ± 13.8
NZS2	126.5 ± 6.6
NZS3	250.8 ± 16.1
NZS4	305.5 ±18.9
NZS5	316.9 ± 13.6
NZS6	337.7 ± 17.9
NZS7	181.8 ± 15.6
NZS8	239.7 ± 17.2
NZS9	194.0 ± 2.5
NZS10	171.7 ± 13.7

APPENDIX 9

Table A11: External Exposure Rates Calculated From Various Concentrations of Terrestrial Radionuclides In Soil (UNSCEAR, 2000).

Radionuclides	Concentration In Soil (Bq/Kg)		Dose Coefficient ($nGyh^{-1}$ per $Bqkg^{-1}$)	Absorbed dose rate in air ($nGyh^{-1}$)	
	Median value	Population weighted average		Median value	Population weighted value
40k	400	420	0.0417	17	18
^{238} U series	35	33	0.462	16	15
^{232} Th series	30	45	0.604	18	27
TOTAL				**51**	**60**

APPENDIX 10

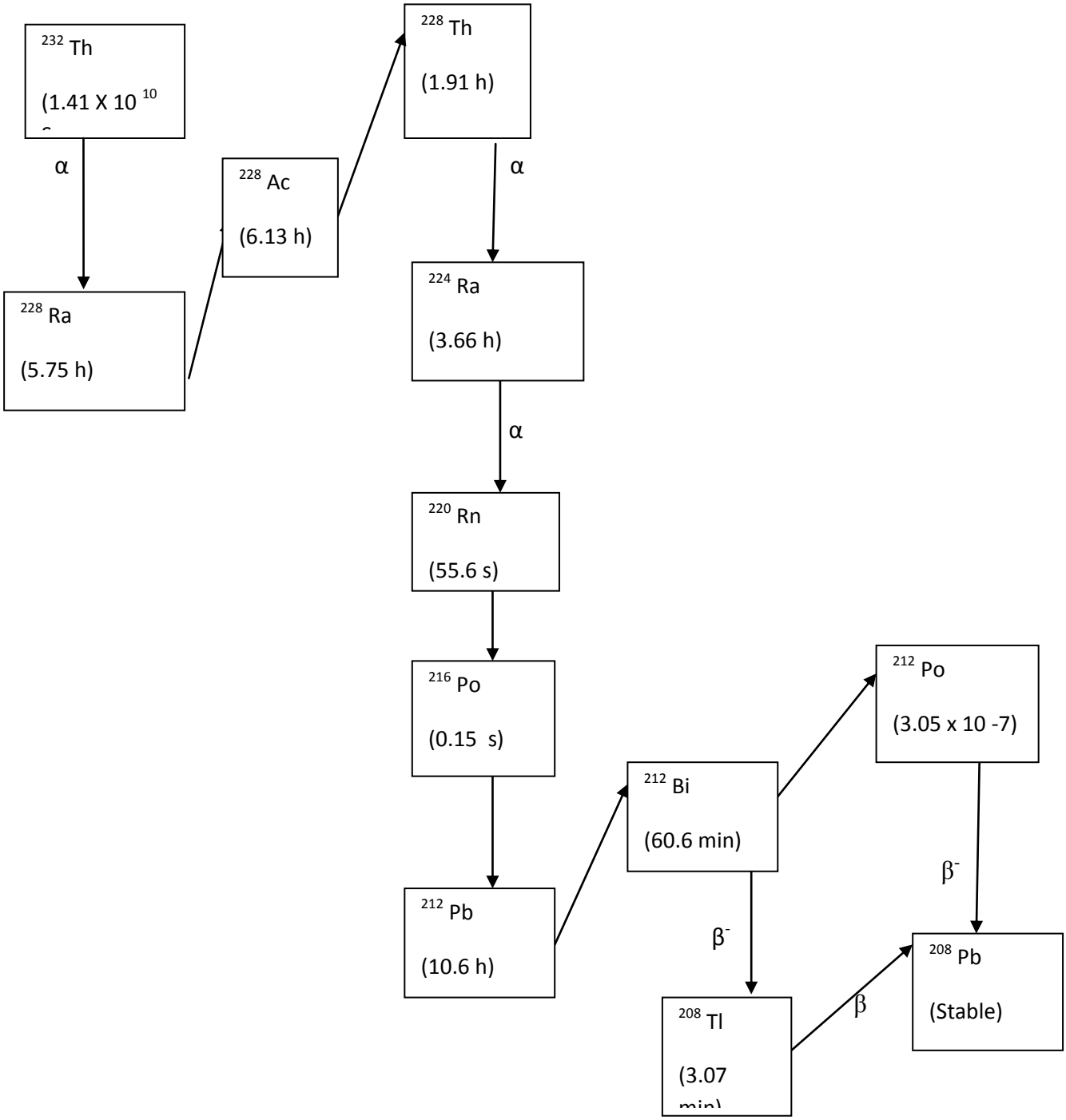

Fig A1: ^{232} Th decay series (UNSCEAR, 1988), ^{208}Tl is radioactive daughter of ^{232} Th.

APPENDIX 11

Table A 12: Radionuclide concentration from other continents (UNSCEAR, 2000)

Region/ Country	Population (1996)<10^6>	Concentration in soil (Bqkg^{-1})					
		^{40}K		^{238}U		^{232}Th	
		MEAN	RAGE	MEAN	RAGE	MEAN	RAGE
Africa							
Algeria	28.78	370	66-1150	30	2-110	25	2-140
Egypt	63.27	320	29-650	37	6-120	18	2-96
N.AMERICA							
Costa Rica	3.50	140	6-380	46	11-130	11	1-42
U.S.A	269.4	370	100-700	35	4-140	35	4-130
E.ASIA							
Bangladesh	120.1	350	130-600				
China	1232	440	9-1800	33	2-690	41	1-360
Hong Kong	6.19	530	80-1100	84	25-130	95	16-200
India	944.6	400	38-760	29	7-81	64	14-160
Japan	125.4	310	15-990	29	2-29	28	2-88
Kazak tan	16.82	300	100-1200	37	12-120	60	10-220
Korea rep.	45.31	670	17-1500				
Malaysia	20.58	310	170-430	66	49-86	82	63-110
Thailand	58.70	230	7-712	114	3-370	51	7-120
W Asia							
Armenia	3.64	360	310-420	46	20-78	30	29-60
Iran	69.98	640	250-980			22	5-42
Syria	14.57	270	87-780	23	10-64	20	10-32
N.Europe							
Denmark	5.24	460	240-610			19	8-30
Estonia	1.47	510	140-1120			27	5-59
Lithuania	3.73	600	350-850	16	3-30	25	9-46
Norway	4.35	850		50		45	
Sweden	8.82	780	560-1150			42	14-94
W.Europe							
Belgium	10.16	380	70-900			27	5-50
Germany	81.92		40-1340		11-330		7-134
Ireland	3.55	350	40-800	37	8-120	26	3-60
Luxembourg	0.41	620	80-1800			50	7-70
Switzerland	7.22	370	40-1000	40	10-150	25	4-70
U.K	58.14		0-3200		2-330		1-180
E.Europe							
Bulgaria	8.47	400	40-800	40	8-190	30	7-160
Hungary	10.05	370	79-570	29	12-66	28	12-45
Poland	38.6	410	110-970	26	5-120	21	4-77
Romania	22.66	490	250-1100	32	8-60	38	11-75
Russia	148.1	520	100-1400	19	0-67	30	2-79
Slovakia	5.35	520	200-1380	32	15-130	38	12-80
S.Europe							
Albania	3.40	360	15-1150	23	6-96	24	4-160
Croatia	4.50	490	140-710	110	83-180	45	12-65
Cyprus	0.76	140	0-670				
Greece	10.49	360	12-1570	25	1-240	21	1-190
Portugal	9.81	840	220-1230	49	26-82	51	22-100
Mean		**420**		**33**		**45**	

APPENDIX 12

Fig A2: Kikuu river Near Nzaui hill.

An aerial photograph showing Kikuu river as it meanders near Nzaui hill in Makueni County (pointed by the arrow) .A River like this one distributes radionuclides contained in the river conglomerates from one area to another.

APPENDIX 13

Fig A3: A display from the survey meter that was used during sampling. It consisted of the Geiger- Müeller Tube and the count meter.

Fig A4: Igneous rocks near Emali town

APPENDIX 14

Fig A5: Rough Bricks made from red soil at Emali town for building and construction in Makueni County.

Fig A6: Hot springs at "Masamukye" in Nguu division in Muooni River.

These hot springs in Fig A6 discharge at the base of the lava. Notice the ripples in the water (circled in red) as the hot springs jet out.